Dietary restriction improves repopulation but impairs lymphoid differentiation capacity of hematopoietic stem cells in early aging

Duozhuang Tang,[1] Si Tao,[1] Zhiyang Chen,[1] Ievgen Oleksandrovich Koliesnik,[1] Philip Gerald Calmes,[1] Verena Hoerr,[3] Bing Han,[1] Nadja Gebert,[1] Martin Zörnig,[4] Bettina Löffler,[3] Yohei Morita,[1] and Karl Lenhard Rudolph[1,2]

[1]Leibniz Institute on Aging, Fritz Lipmann Institute (FLI), 07745 Jena, Germany
[2]Faculty of Medicine, Friedrich Schiller University, 07743 Jena, Germany
[3]Institute of Medical Microbiology, Jena University Hospital, 07743 Jena, Germany
[4]Georg Speyer Haus, Institute for Tumor Biology and Experimental Therapy, 60596 Frankfurt am Main, Germany

Dietary restriction (DR) improves health, delays tissue aging, and elongates survival in flies and worms. However, studies on laboratory mice and nonhuman primates revealed ambiguous effects of DR on lifespan despite improvements in health parameters. In this study, we analyzed consequences of adult-onset DR (24 h to 1 yr) on hematopoietic stem cell (HSC) function. DR ameliorated HSC aging phenotypes, such as the increase in number of HSCs and the skewing toward myeloid-biased HSCs during aging. Furthermore, DR increased HSC quiescence and improved the maintenance of the repopulation capacity of HSCs during aging. In contrast to these beneficial effects, DR strongly impaired HSC differentiation into lymphoid lineages and particularly inhibited the proliferation of lymphoid progenitors, resulting in decreased production of peripheral B lymphocytes and impaired immune function. The study shows that DR-dependent suppression of growth factors and interleukins mediates these divergent effects caused by DR. Supplementation of insulin-like growth factor 1 partially reverted the DR-induced quiescence of HSCs, whereas IL-6/IL-7 substitutions rescued the impairment of B lymphopoiesis exposed to DR. Together, these findings delineate positive and negative effects of long-term DR on HSC functionality involving distinct stress and growth signaling pathways.

Experimental dietary restriction (DR) is based on a 10–30% reduction in food intake without leading to malnutrition (Omodei and Fontana, 2011). DR has been intensively studied and was shown to elongate the lifespan of *Caenorhabditis elegans*, *Drosophila melanogaster*, and rats (Fontana et al., 2010). Studies on inbred laboratory mice revealed that DR elongates lifespan in some mouse strains, whereas in others, the effects of DR were neutral or even resulted in lifespan shortening compared with ad libitum (AL)–fed controls (Harper et al., 2006). In long-lived nonhuman primates, two studies reported on the consequences of long-term DR on overall lifespan (Colman et al., 2009; Mattison et al., 2012). In both studies, DR did not result in a significant elongation of the lifespan compared with AL controls when all primates were included in the analysis (Colman et al., 2009; Mattison et al., 2012). These results stand in contrast to multiple studies having unambiguously documented beneficial effects of DR on health parameters and disease prevention in both murine models and primates, including suppression of cancer development, memory loss, hearing impairments, type 2 diabetes, hypertension, and heart disease (Shimokawa et al., 1993; Mattson, 2005; Cohen et al., 2009; Colman et al., 2009; Omodei and Fontana, 2011; Mattison et al., 2012).

To better understand the effects of DR on health and lifespan, it is important to characterize the cellular consequences of DR at the level of adult tissue stem cells. Adult stem cells exist in many mammalian organs and tissues. Given that stem cells play essential roles in the maintenance of tissue homeostasis and tissue regeneration after damage, it is believed that age-related changes in stem cell function impact tissue aging (Dorshkind et al., 2009; Jones and Rando, 2011; Goldberg et al., 2015). Indeed, age-related declines in stem cell functionality occur in various tissues (Liu and Rando,

Correspondence to Yohei Morita: yohei.morita@leibniz-fli.de; or Karl Lenhard Rudolph: lenhard.rudolph@leibniz-fli.de

D. Tang's present address is Dept. of Hematology, The Second Affiliated Hospital of Nanchang University, 330006 Nanchang, China.

S. Tao's present address is Dept. of Oncology, The Second Affiliated Hospital of Nanchang University, 330006 Nanchang, China.

Abbreviations used: ADX, adrenalectomy; AL, ad libitum; CLP, common lymphoid progenitor; CMP, common myeloid progenitor; DR, dietary restriction; GMP, granulocyte/macrophage progenitor; HSC, hematopoietic stem cell; MEP, megakaryocyte/erythrocyte progenitor; PB, peripheral blood; proEry, proerythroblast; qRT-PCR, quantitative real-time PCR; RF, refeeding.

The Rockefeller University Press $30.00
J. Exp. Med. 2016 Vol. 213 No. 4 535–553
www.jem.org/cgi/doi/10.1084/jem.20151100

2011). However, the effects of DR on stem cell functionality and aging remain to be characterized in greater detail. It was reported that DR enhances muscle stem cell maintenance and activity to regenerate damaged muscle (Cerletti et al., 2012). In addition, it was shown that DR augments stem cell activity in the intestinal epithelium by stimulating mammalian target of rapamycin complex 1 (mTORC1) signaling in the Paneth cells that form a niche for intestinal stem cells (Yilmaz et al., 2012).

In the hematopoietic system, DR ameliorated aging-associated increases in the self-renewal of phenotypic hematopoietic stem cells (HSCs) with reduced functionality as well as defects in the clearance of nonproliferative (senescent) and damaged T lymphocytes (Spaulding et al., 1997a; Chen et al., 1998, 2003; Ertl et al., 2008). However, DR-fed mice exhibited an enhanced susceptibility to infections indicative of impaired immune functions (Peck et al., 1992; Gardner, 2005; Kristan, 2007; Goldberg et al., 2015). Mechanistically, the effects of DR on HSC functionality remain incompletely understood but are influenced by genetic factors (Ertl et al., 2008).

In this study, we analyzed the short- and long-term effects of adult-onset 30% DR on the capacity of HSCs and progenitor cells in maintaining hematopoietic repopulation and B lymphopoiesis in C57BL/6J mice. The study provides the first experimental evidence that long-term DR alters the lymphoid cell differentiation potential of HSCs and progenitor cells, resulting in immune defects in the context of prolonged bacterial infection. However, long-term DR from young adulthood to midlife improves the maintenance of the repopulation capacity of HSCs by enhancing stem cell quiescence. The study identifies distinct stress signaling factors (IL-6 and IL-7) and growth factors (insulin-like growth factor 1 [IGF1]) that contribute to both the positive and adverse effects of DR on HSC functionality.

RESULTS

DR retards HSC aging

HSC aging is characterized by increases in the overall pool size of HSCs but decreases in the capacity of HSCs in maintaining hematopoietic repopulation and lymphopoiesis. This associates with a shift in the HSC pool characterized by substantially increasing numbers of myeloid-biased HSCs that predominantly generate myeloid lineages, but relatively little increases in lymphoid-biased HSCs that predominantly generate lymphoid lineages. This shift in the HSC population is thought to contribute to myeloid skewing of blood cells and decreases in immune functions in response to aging (Morrison et al., 1996; de Haan et al., 1997; Chen et al., 1999; Rossi et al., 2005; Chambers and Goodell, 2007; Beerman et al., 2010; Florian et al., 2012; Geiger et al., 2013). To analyze the long-term consequences of an adult-onset DR on HSCs during aging, 3-mo-old mice were treated with a 30% DR, and analysis of HSC number was followed regularly after up to 9 mo of the treatment. Although the study period ended in midlife (12 mo old) mice, HSCs of mice from the AL group already developed typical phenotypes of aging, e.g., an increase in HSC numbers and a skewing toward myeloid-biased HSCs. Intriguingly, although the phenotypically defined HSCs ($CD150^+CD34^-c\text{-}Kit^+Sca\text{-}1^+lineage^-$ cells = $CD150^+CD34^-KSL$) increased by approximately fivefold in the AL mice at the age of 12 mo, they increased only very mildly in DR mice (Fig. 1 A). Furthermore, the increase of myeloid-biased HSCs ($CD150^{hi}CD34^-KSL$) and the imbalance of the HSC pool in AL mice were substantially rescued in DR mice maintaining a balanced HSC pool at the age of 12 mo (Fig. 1, B and C; and Fig. S1). To further study the influence of DR on HSC function, transplantation experiments were conducted after mid- (6 mo) and long-term (1 yr) DR versus AL diet. Highly purified phenotypic HSCs ($CD150^+CD34^-KSL$) derived from the DR- or AL-treated mice were transplanted along with competitor cells. Interestingly, DR donor–derived HSCs showed a significantly stronger repopulating capacity compared with AL donor–derived HSCs (Fig. 1, D–I). Moreover, serial transplantation experiments revealed improved self-renewal capacity of HSCs derived from DR donors compared with HSCs from AL donors (Fig. 1, I and J). Together, these data indicated that DR leads to improved maintenance of the functional reserve of HSCs during aging. An analysis of the lineage chimerism from donor-derived HSCs revealed that DR donor–derived HSCs had a greatly enhanced lymphoid output compared with AL donor–derived HSCs starting as early as 3–4 wk after transplantation (Fig. 1, E, F, H, and I). This improvement in DR donor–derived repopulation capacity was less pronounced in the myeloid lineage (Fig. 1, G–I), but in line with the overall increase in repopulation capacity, DR donor–derived HSCs also exhibited an increase in myeloid output at later time points after transplantation (Fig. 1 G). Together, these data showed that DR not only phenotypically maintained a balanced myeloid/lymphoid ratio within the HSC pool but also the potential of the HSC pool to generate cells of lymphoid lineage.

DR increases HSC quiescence

It is believed that quiescence is a key mechanism contributing to the prevention of aging- and proliferation-induced declines in HSC functionality. Although the majority of adult HSCs are resting under physiological status, they regularly enter and exit the cell cycle to produce short-lived downstream cells in 2–3-mo intervals (Wilson et al., 2008; Sun et al., 2014; Busch et al., 2015). These rounds of cell division are thought to contribute to the loss of HSC functionality during aging (Passegué et al., 2005; Beerman et al., 2013; Flach et al., 2014; Walter et al., 2015). HSCs do not have an unlimited capacity of self-renewal, which is known to exhaust within four to six rounds of serial transplantation–induced replication stress. Increased HSC cycling was shown to lead to the loss of stem cell activity in many genetically modified mouse models (El-Deiry et al., 1993; Cheng et al., 2000; Lee and Yang, 2001; Hock et al., 2004; Yilmaz et al., 2006; Zhang et

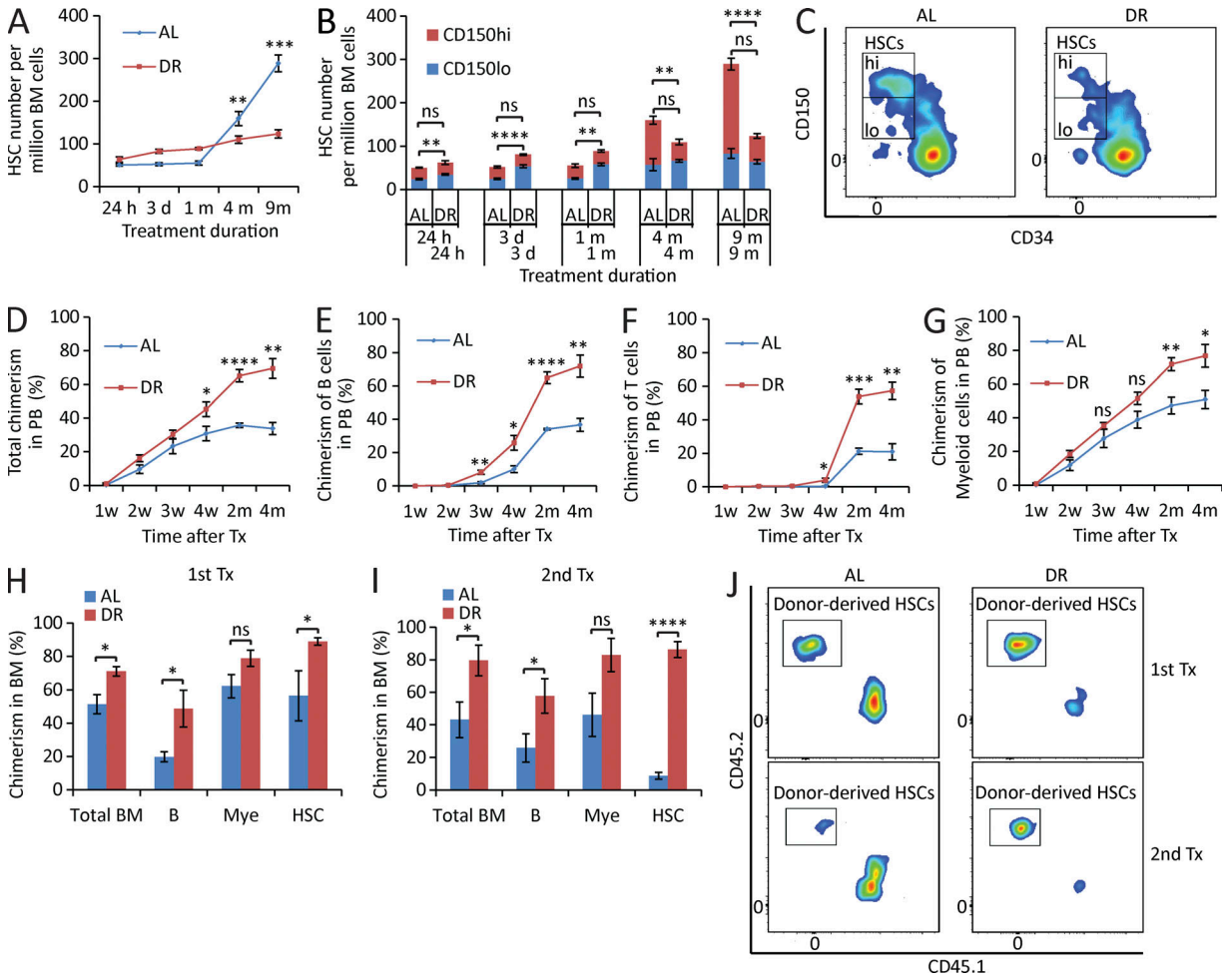

Figure 1. **DR retards HSC aging.** (A–C) 3-mo-old mice were fed with DR diet or AL diet. The HSC population was analyzed by flow cytometry at the indicated time points after dietary intervention (n = 3–5 mice per group per time point; n = 2 independent experiments). Note that the number of HSCs, in particular myeloid-biased HSCs, of DR mice was maintained relatively stable, whereas it increased significantly over time during aging in AL mice. In B, the significance of the comparison was shown in the lower line for the lymphoid-biased HSCs ($CD150^{lo}$ HSCs) and in the upper line for the myeloid-biased HSCs ($CD150^{hi}$ HSCs). Note that the skewing toward myeloid-biased HSCs during aging in AL mice was rescued in DR mice. (C) Representative FACS plots of mice treated with 9-mo DR or AL gated from c-$Kit^+$$Sca\text{-}1^+$lineage$^-$ BM cells. (D–G) 100 HSCs derived from donor mice treated with mid-term (6 mo) DR or AL were transplanted along with 2 × 10^5 total BM cells from competitor mice into recipient mice (n = 4–5 mice per group; n = 2 independent experiments). Panels show donor-derived total chimerisms (D), chimerisms of lymphoid lineage (E and F), and chimerisms of myeloid lineage (G) in PB at the indicated time points after transplantation. (H–J) 200 HSCs derived from donor mice treated with long-term (1 yr) DR or AL were transplanted along with 2 × 10^5 total BM cells from competitor mice into recipient mice. 4 mo later, 10^7 BM cells from the primary recipients were transplanted to secondary recipient mice (n = 4–5 mice per group; n = 2 independent experiments). (H and I) Donor-derived chimerisms in BM 4 mo after primary (H) and secondary (I) transplantation (Tx). (J) Representative FACS plots of primary and secondary recipient mice gated from HSCs. HSCs, $CD150^+CD34^-$c-$Kit^+$$Sca\text{-}1^+$lineage$^-$ BM cells; m, months; B, B cells; T, T cells; Mye, myeloid cells; w, weeks. Data are displayed as mean ± SEM. *, $P < 0.05$; **, $P < 0.01$; ***, $P < 0.001$; ****, $P < 0.0001$ by unpaired two-tailed Student's t test. ns, not significant.

al., 2006; Orford and Scadden, 2008). To test whether DR influences the quiescence of HSCs, the cell cycle status was analyzed by flow cytometry under DR condition. Notably, HSCs exhibited a fast response to DR, leading to a significant increase in the percentage of quiescent HSCs (in G0 phase) appearing 3 d after initiation of DR (Fig. 2 A). This increase in quiescent HSCs persisted as the treatment was applied for a longer period (Fig. 2, A and B). Continuous BrdU labeling—a protocol known to push HSCs into cell cycle (Wilson et al., 2008)—provoked strong increases in HSC cycling in AL-fed control mice (Fig. 2, C and D). Of note, DR impaired the responsiveness of HSCs to BrdU-induced cell cycle activity (Fig. 2, C and D). To further test whether DR reduces HSC proliferation in response to stress, polyinosinic-polycytidylic acid (pIpC)—a known activator of interferon signaling—was injected to DR or AL pretreated mice, and HSC cell cycle activity was analyzed 16 h after injection. Consistent with a previous study (Essers et al., 2009), pIpC significantly activated

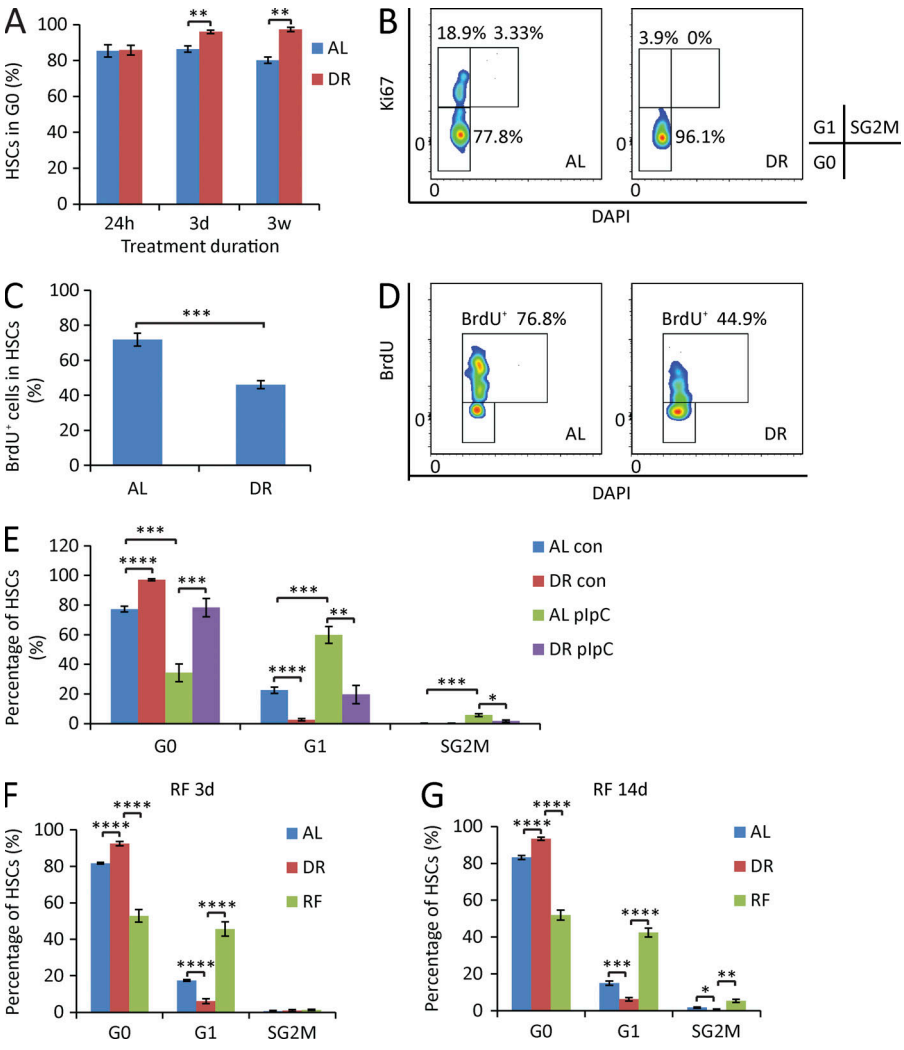

Figure 2. **DR increases HSC quiescence.** (A and B) HSCs were freshly isolated from mice that were treated for the indicated time periods with a DR or AL diet. Cell cycle was analyzed by FACS using Ki67 and DAPI staining (n = 3–5 mice per group per time point; n = 2 independent experiments). (A) Quantification of HSCs in G0 phase. Unpaired two-tailed Student's t test was used. (B) Representative FACS plots gated from HSCs of mice treated with DR or AL for 3 wk. (C and D) Mice were treated with DR or AL for 10 d. On day 4, a single dose of 180 µg BrdU was injected intraperitoneally, and the mice were continuously supplied with 0.8 mg/ml BrdU in drinking water for the subsequent 6 d (n = 5 mice per group per time point; n = 2 independent experiments). (C) Quantification of BrdU-incorporated HSCs on day 10 (6 d after bolus injection followed by continuous supplementation of BrdU). Unpaired two-tailed Student's t test was used. (D) Representative FACS plots gated from HSCs. (E) Mice were treated with DR or AL for 8 d followed by a single 5-mg/kg dose of pIpC injection. 16 h after injection, HSC cell cycle activity was analyzed by flow cytometry by Ki67 and DAPI staining (n = 4–5 mice per group per time point; n = 2 independent experiments). One-way ANOVA analysis was used. (F and G) Mice were treated with DR or AL for 3 wk. Afterward, half of the mice in the DR group were refed AL (RF), whereas the remaining mice were continuously treated with the same diet as before. HSC cycle activity from all groups was analyzed 3 d (F) and 14 d (G) after RF by flow cytometry using Ki67 and DAPI staining (n = 4–5 mice per group per time point; n = 2 independent experiments). One-way ANOVA analysis was used. Note that HSC cycle activity was strongly activated upon RF. Data are displayed as mean ± SEM. *, $P < 0.05$; **, $P < 0.01$; ***, $P < 0.001$; ****, $P < 0.0001$. ns, not significant.

HSCs in AL mice (Fig. 2 E). Although responsive to pIpC, HSCs of DR mice remained significantly more quiescent compared with HSCs of AL mice (Fig. 2 E). Together, these findings indicated that DR increases HSC quiescence and reduces HSC proliferation in response to stress.

To further investigate how dietary modulation regulates HSC cell cycle activity, mice were kept on DR for 3 wk and then reexposed to an AL diet (refeeding [RF]). Reaccess to an AL diet led to a quick (within 3 d) and overshooting G1 entry of HSCs, which by far exceeded the percentage of G1 phase HSCs in mice that were permanently exposed to an AL diet (Fig. 2 F). This increase in HSC cycling was still seen at 14 d of RF (Fig. 2 G). Together, these data revealed a DR-dependent switch of HSCs from proliferation into quiescence, which is revertible by RF.

DR leads to suppression of B lymphopoiesis and enhanced erythropoiesis/myelopoiesis

The aforementioned data indicated that DR prevents aging-associated increases in the self-renewal of myeloid-biased HSCs ($CD150^{hi}CD34^{-}KSL$) but to a much lesser extent in lymphoid-biased HSCs with low CD150 expression ($CD150^{lo}CD34^{-}KSL$), thus preventing myeloid skewing of the HSC pool during aging (Fig. 1 B). To directly address whether DR would also rescue the skewing of hematopoiesis at the progenitor and differentiated blood cell level, different hematopoietic lineages were analyzed kinetically by flow cytometry in adult-onset DR mice compared with AL-fed control mice. In contrast to the beneficial effects at the HSC level, DR showed a significant adverse effect on B lymphopoiesis, indicating a dual role of DR in hematopoietic homeostasis. DR had no strong effect on the overall cell number of hematopoietic

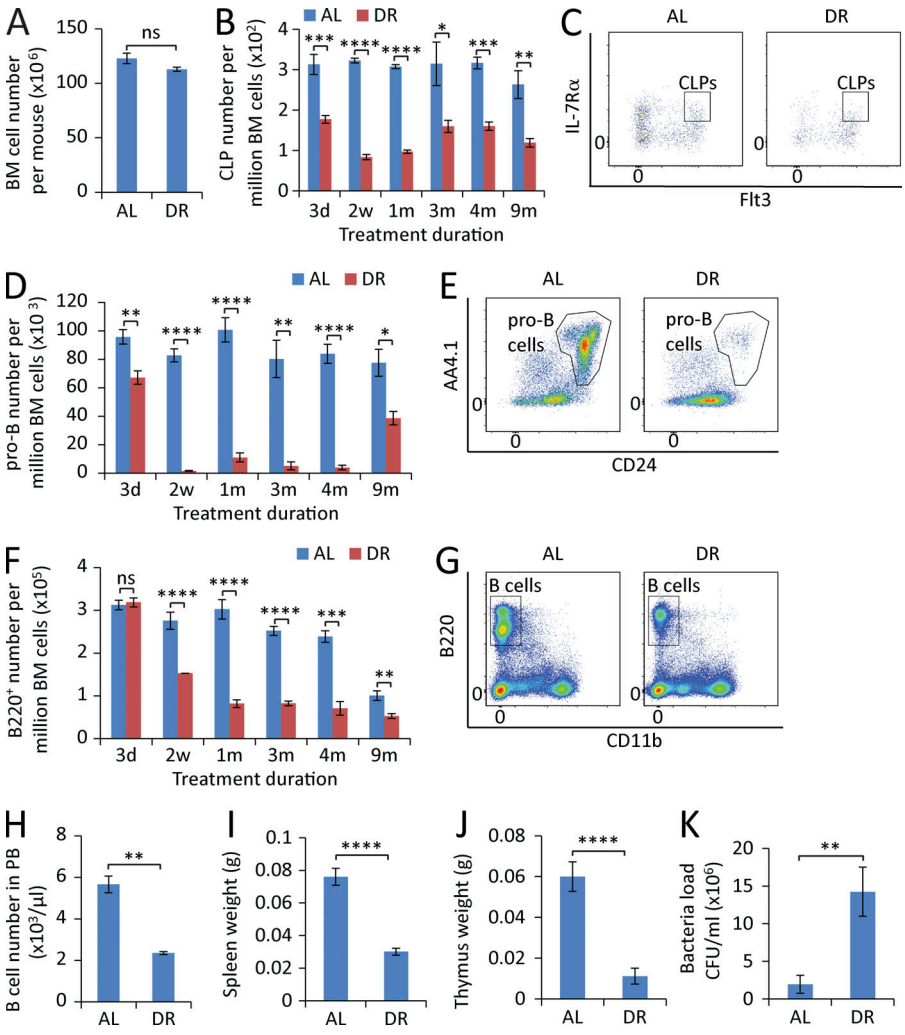

Figure 3. **DR leads to a sequential reduction of lymphopoiesis in BM.** (A) Total number of BM cells of mice treated with DR or AL for 2 wk (n = 5 mice per group; n = 2 independent experiments). (B, D, and F) Flow cytometry analysis of CLPs (B), pro–B cells (D), and B220$^+$ cells (F) of BM from mice treated with DR or AL for the indicated time periods (n = 4–5 mice per group per time point; n = 2 independent experiments). Note a sequential reduction from early progenitors to downstream differentiated cells. (C, E, and G) Representative FACS plots at 2-wk time point gated from c-Kit$^{mid/low}$Sca-1$^{mid/low}$lineage$^-$ cells (C), B220$^+$TER-119$^-$Gr-1$^-$CD11b$^-$CD3$^-$ cells (E), and total BM cells (G). (H–J) B cell counting in PB (H), spleen weight (I), and thymus weight (J) of mice treated with DR or AL for 2 wk (n = 5 mice per group; n = 2 independent experiments). (K) Mice were treated with a DR or AL diet for 10 d and injected with bacteria or vehicle control in the feet. Bacterial load was measured 1 wk after the bacterial injection (n = 6 mice per group; n = 2 independent experiments). CLPs, IL-7Rα$^+$Flt3$^+$c-Kit$^{mid/low}$ Sca-1$^{mid/low}$ lineage$^-$ cells; pro-B cells, B220$^+$ CD24$^+$AA4.1$^+$TER-119$^-$Gr-1$^-$CD11b$^-$CD3$^-$ cells. Data are displayed as mean ± SEM. *, P < 0.05; **, P < 0.01; ***, P < 0.001; ****, P < 0.0001 by unpaired two-tailed Student's t test. ns, not significant.

cells in BM (Fig. 3 A). However, it induced a severe impairment of B lymphopoiesis (Fig. 3, B–G). The reduction of B lymphopoiesis did not occur in all lymphoid subpopulations simultaneously, but affected the lineage in a sequential manner starting at early progenitor cell level and then going stepwise down the lineage toward mature B lymphocytes. Specifically, within 3 d of DR, the frequency of common lymphoid progenitors (CLPs; IL-7Rα^{+}Flt3$^+$c-Kit$^{mid/low}$Sca-1$^{mid/low}$lineage$^-$ cells; see Fig. S2 for representative gating strategy) dropped by 50% (Fig. 3, B and C), and pro–B cells (B220$^+$CD24$^+$AA4.1$^+$TER-119$^-$Gr-1$^-$CD11b$^-$CD3$^-$; Fig. S3) decreased by ∼25% (Fig. 3, D and E), whereas mature B cell numbers in BM remained unchanged at this time point (Fig. 3 F). Notably, longer treatment of DR (2 wk) resulted in a striking diminishment of lymphoid progenitors (Fig. 3, B–E) and a significant decrease of mature B cells in the BM (Fig. 3, F and G) as well as in the peripheral blood (PB; Fig. 3 H), accompanied by a remarkable shrinkage of spleen and thymus (Fig. 3, I and J) and a significant impairment of bacteria clearance upon infection challenge (Fig. 3 K). When DR persisted >9 mo, a recovery of pro–B cell population occurred, but still remained reduced compared with AL mice (Fig. 3 D). Throughout the investigation period (up to 9 mo of the treatment), the B lymphoid lineage was maintained at a significantly smaller volume compared with the AL mice (Fig. 3 F).

In contrast to the suppression of B lymphopoiesis, erythropoiesis and myelopoiesis were enhanced in DR-treated mice. The number of common myeloid progenitors (CMPs; CD16/32$^-$CD34$^+$c-Kit$^+$Sca-1$^-$lineage$^-$ cells; Fig. S1), megakaryocyte/erythrocyte progenitors (MEPs; CD16/32$^-$CD34$^-$c-Kit$^+$Sca-1$^-$lineage$^-$ cells; Fig. S1), granulocyte/macrophage progenitors (GMPs; CD16/32$^+$CD34$^+$c-Kit$^+$Sca-1$^-$lineage$^-$ cells; Fig. S1), proerythroblasts (proEry's; CD71$^+$TER-119^{mid} cells; Fig. S4), and CD11b$^+$ myeloid cells were all elevated in the BM of DR mice (Fig. 4, A–G). In line with the increase of erythroid progenitor cells, RBCs and hemoglobin were significantly increased in the PB of DR mice (Fig. 4, H and I). The increase in erythropoiesis in response to DR persisted throughout the observation period (up to 9 mo of DR) and was more prominent than the increase in myelopoiesis (Fig. 4, B, D, H, and I), suggesting that DR induces a biased hematopoiesis mainly toward erythropoiesis.

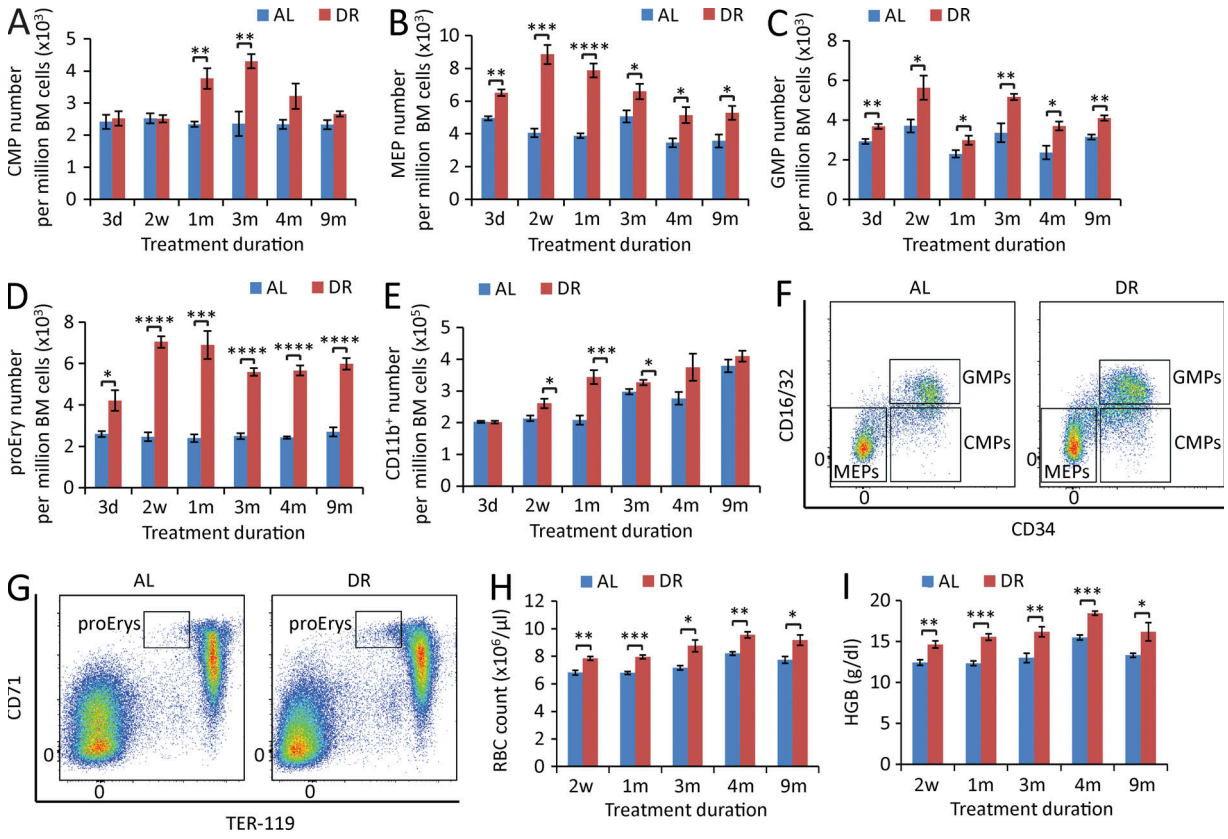

Figure 4. **DR leads to enhanced erythropoiesis and myelopoiesis in BM.** (A–E) Flow cytometry analysis of CMPs (A), MEPs (B), GMPs (C), proEry's (D), and myeloid cells (E) of BM from mice treated with DR or AL for the indicated time periods (n = 4–5 mice per group per time point; n = 2 independent experiments). (F and G) Representative FACS plots at 2-wk time point gated from c-Kit⁺Sca-1⁻lineage⁻ cells (F) and total BM cells (G). (H and I) PB cell counting of RBC (H) and hemoglobin (I) of mice treated with DR or AL for the indicated time periods (n = 4–5 mice per time point per group; n = 2 independent experiments). CMPs, CD16/32⁻CD34⁺c-Kit⁺Sca-1⁻lineage⁻ cells; MEPs, CD16/32⁻CD34⁻c-Kit⁺Sca-1⁻lineage⁻ cells; GMPs, CD16/32⁺CD34⁺c-Kit⁺Sca-1⁻lineage⁻ cells; proEry's, CD71⁺TER-119^{mid} cells; HGB, hemoglobin. Data are displayed as mean ± SEM. *, P < 0.05; **, P < 0.01; ***, P < 0.001; ****, P < 0.0001 by unpaired two-tailed Student's t test. ns, not significant.

Interestingly, the RF of an AL diet to mice that were kept for 3 wk on DR led to a strong recovery of B lymphoid lineage, again proceeding in a sequential stepwise process with the fastest response in CLPs followed by recovery of pro–B cells and mature B220⁺ cells in BM (Fig. 5, A–C). RF induced a transiently overshooting recovery response characterized by a sequential occurrence of super-normal cell numbers (higher than in control mice that were continuously kept on AL diet) first affecting CLPs, followed by pro–B cells and then by B220⁺ cells (Fig. 5, A–C). The overshooting recovery response of CLPs was down-regulated to subnormal cell numbers when overproduction of downstream pro–B and mature B220⁺ cells became apparent (Fig. 5, A–C). It is possible that this overshooting response to RF also contributed to the strong enhancement of lymphopoiesis at early time points after transplantation of DR donor–derived HSCs compared with AL donor–derived HSCs into lethally irradiated AL recipients (Fig. 1, E and F).

DR impairs differentiation of lymphoid-biased HSCs and early progenitor cells

The aforementioned findings indicated that DR rescues aging-induced skewing within the HSC pool by ameliorating the aging associated increase in myeloid-biased HSCs (CD150^{hi}). The myeloid skewing of the aging HSC pool is thought to contribute to aging-induced impairments in lymphopoiesis and immune function (Wang et al., 2011). Although DR ameliorated myeloid skewing of the HSC pool, DR did not result in improved but impaired lymphopoiesis and reduced immune function (Fig. 3). These data prompted an investigation of the effects of DR on the lymphoid cell differentiation potential of HSCs and early progenitor cells. As currently understood, CLPs and CMPs have very limited or no self-renewal activity and must be continuously replenished by differentiation of HSCs. Analyzing the ratio of CLPs to lymphoid-biased HSCs and the ratio of pro–B cells to CLPs revealed a significant reduc-

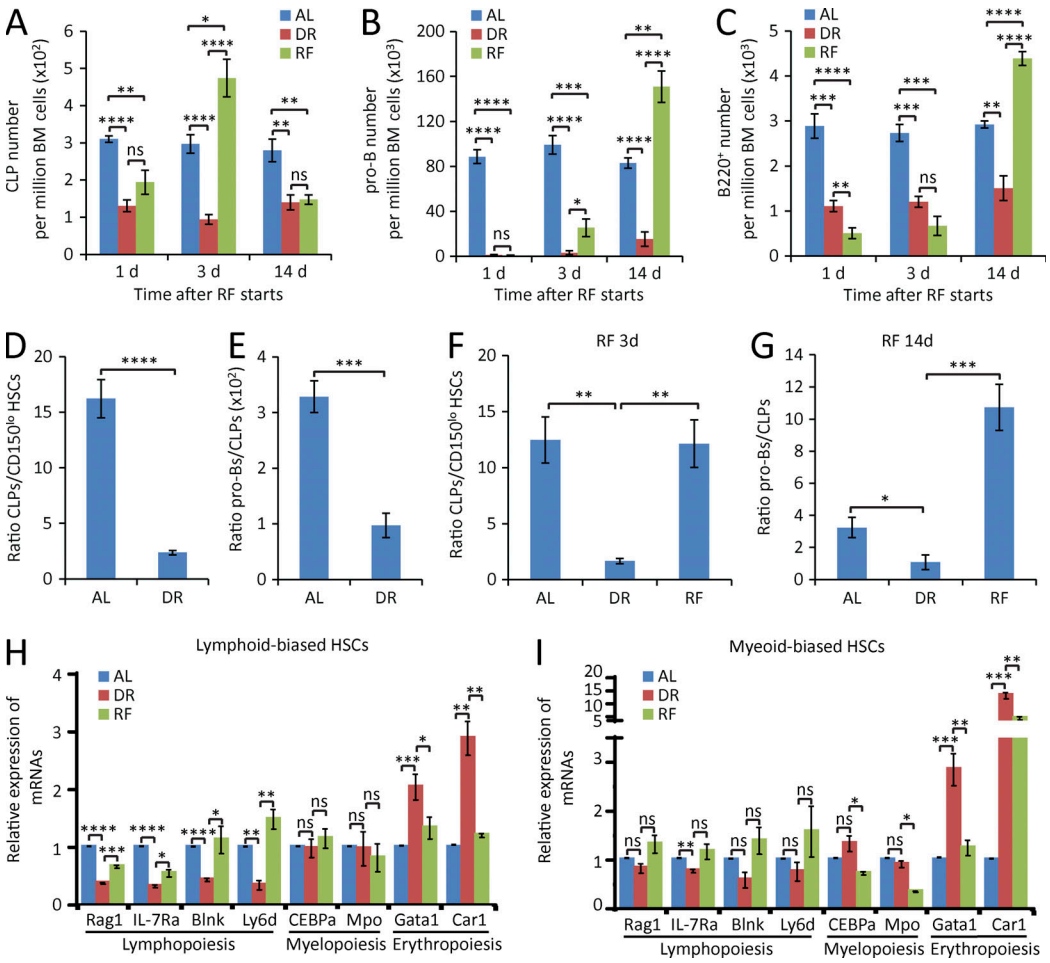

Figure 5. **DR impairs lymphoid cell differentiation and enhances erythropoiesis in lymphoid-biased HSCs.** (A–C) Mice were treated with DR or AL for 3 wk. Afterward, half of the mice in the DR group were refed AL (RF), whereas the remaining mice were continuously treated with the same diet as before. The numbers of CLPs (A), pro–B cells (B), and B220⁺ cells (C) in BM were analyzed by flow cytometry at the indicated time points after RF (n = 5 mice per group per time point; n = 2 independent experiments). One-way ANOVA analysis was used. Note that a sequential recovery occurred first in CLPs, second in pro–B cells, and lastly in B220⁺ cells after RF. (D and E) Flow cytometry analysis of the ratio of CLPs versus lymphoid-biased HSCs (D) and pro–B cells versus CLPs (E) of BM from mice treated with DR or AL for 1 mo (n = 5 mice per group; n = 2 independent experiments). Unpaired two-tailed Student's t test was used. (F–I) Mice were treated with DR or AL for 3 wk. Afterward, half of the mice in the DR group were refed AL for 3 or 14 d, whereas the remaining mice were continuously treated with the same diet as before (n = 5 mice per time point per group; n = 2 independent experiments). One-way ANOVA analysis was used. (F) Ratio of CLPs versus lymphoid-biased HSCs after RF for 3 d. (G) Ratio of pro–B cells versus CLPs after RF for 14 d. (H and I) The expressions of lymphoid-, myeloid-, and erythroid-specific genes in lymphoid-biased HSCs (H) and myeloid-biased HSCs (I) were analyzed by qRT-PCR after RF for 3 d (n = 3 independent experiments). For each experiment, HSCs were obtained from a pool of three to four mice per group. Data are displayed as mean ± SEM. *, P < 0.05; **, P < 0.01; ***, P < 0.001; ****, P < 0.0001. ns, not significant.

tion of these ratios in response to DR (Fig. 5, D and E). Interestingly, RF rescued the skewed ratio of CLPs versus lymphoid-biased HSCs as well as the ratio of pro–B cells versus CLPs (Fig. 5, F and G). These data indicated that DR significantly compromised the lymphoid cell differentiation capacity of lymphoid-biased HSCs and early lymphoid progenitor cells. Of note, these inhibitory effects outweighed the positive effect of DR on preventing aging-associated myeloid skewing of the HSC pool (Figs. 1 and 3), resulting in an overall reduction of peripheral lymphocytes in blood and lymphoid organ (Fig. 3, H–J).

DR impairs master regulators of lymphoid cell differentiation in lymphoid-biased HSCs and proliferation of CLPs

Fate- and lineage-specifying genes are known to precede lineage commitment at multipotent stages (Miyamoto et al., 2002). Lineage commitment of HSCs is regulated by the expression of lineage-specific genes (Cheng et al., 1996; Kondo et al., 1997; Muller-Sieburg et al., 2004). To directly test whether DR-induced alterations in HSC differentiation were mediated by cell-intrinsic alteration in the expression of key regulators of myeloid/erythroid versus lymphoid cell differentiation, the

expression of candidate genes was analyzed in purified HSC populations by real-time PCR. Intriguingly, lymphoid-biased HSCs exhibited a significant inhibition of lymphoid-specific genes (*Blnk*, *Rag1*, *IL-7Rα*, and *Ly6d*) and an induction of erythroid-specific genes (*Gata1* and *Car1*) in DR-fed mice compared with AL-fed mice (Fig. 5 H). In contrast, myeloid-biased HSCs did not show strong alterations in the expression of lymphoid cell differentiation–inducing genes in response to DR (Fig. 5 I). However, myeloid-biased HSCs exhibited a significant induction of erythroid cell differentiation–inducing genes in response to DR, indicating that myeloid-biased HSCs contributed to the increase in erythroid cells under DR conditions. RF of the mice rescued these alterations in the gene expression in lymphoid-biased and myeloid-biased HSCs (Fig. 5, H and I). Myeloid-specific genes (*CEBPα* and *Mpo*) were not significantly changed in either lymphoid-biased or myeloid-biased HSCs in response to DR, but were significantly down-regulated in myeloid-biased HSCs upon RF (Fig. 5, H and I). These data suggested that DR induces alterations in differentiation program in HSCs, mainly involving suppression of lymphoid cell differentiation in lymphoid-biased HSCs and enhancement of erythroid cell differentiation in myeloid-biased HSCs and lymphoid-biased HSCs.

To test additional mechanisms that could be involved in the skewed hematopoiesis under DR conditions, cell cycle status and proliferation were analyzed at early progenitor cell stages (CLPs, MEPs, GMPs, and CMPs). The analyses uncovered that DR elevated the number of CLPs in quiescence (Fig. 6, A–G), whereas RF stimulated the cell cycle activity of CLPs to enter G1 phase (Fig. 6, F and G). These results indicated that DR inhibits the cell cycle progression and the proliferation of CLPs. In contrast to the result on CLPs, DR did not suppress cell cycle activity of MEPs, GMPs, or CMPs but led to mild increases in cell cycle activity in the population MEPs and GMPs (Fig. 6, H–J), which was diminished by RF (Fig. 6, H and I). However, the effect size of these dietary-induced changes in cell cycle activity was very small in these progenitor cell populations, suggesting that DR-dependent increases in erythroid output likely involve proliferation-independent mechanisms, such as changes in differentiation of HSCs and early progenitor cells, resulting in the generation of higher numbers of MEPs and proEry's producing a higher erythroid output with albeit marginally enhanced proliferation rates.

To further analyze DR-mediated effects on the reduction of CLPs in BM, CLP migration and apoptosis were analyzed. DR did not change the rate of CLP migration to spleen (Fig. 7 A), the rate of CLP apoptosis (Fig. 7 B), or the expression of apoptosis-inducing genes in CLPs (Fig. 7 C). Because p53 is a regulator of apoptosis, cell cycle, and differentiation of HSCs (Kastan et al., 1991; Liu et al., 2009), we performed DR on 2-mo-old p53 knockout ($p53^{-/-}$) mice and $p53^{+/+}$ littermate controls. p53 deletion did not rescue DR-induced reductions in the number of CLPs (Fig. 7 D), pro–B cells, or $B220^{+}$ cells (not depicted). Moreover, p53 gene status did not affect DR-mediated suppression of cell cycle activity and expression of lymphoid-specific genes in lymphoid-biased HSCs (Fig. 7, E and F). Also, the deletion of Puma (the primary mediator of p53 dependent apoptosis; Jeffers et al., 2003) or the overexpression of Bcl2 (an inhibitor of apoptosis; Ogilvy et al., 1999) did not rescue the decrease in the number of CLPs (Fig. 7, G and H), pro–B cells, or $B220^{+}$ cells (not depicted) in response to DR conditions. Collectively, these data indicated that DR-mediated decreases in lymphopoiesis were not mediated by apoptosis but involved p53-independent suppression of cell cycle activity of HSCs as well as p53-independent alterations in the differentiation of HSCs.

DR-mediated suppression of IGF1 contributes to increases in HSC quiescence but not the skewing of HSC differentiation

The aforementioned findings indicated that DR prevents aging-induced myeloid skewing within the HSC pool but at the same time strongly impairs the lymphoid cell differentiation capacity of HSCs and CLPs, whereas differentiation of HSCs into erythroid/myeloid cells is maintained at high levels irrespective of dietary regiments. It is known that DR suppresses several systemic factors, including growth factors and inflammatory factors. The data on cell cycle analysis and apoptosis suggested that DR-induced increases in G0 residency could contribute to this impairment in differentiation. Because systemic factors are known regulators of HSC activity (Ju et al., 2007; Song et al., 2012), we sought to test whether alteration in systemic factors mediates the roles of DR on hematopoiesis. To this end, we studied the outcome of supplementing several systemic acting factors in mice exposed to DR. The liver senses the nutrient status and regulates energy metabolism, cell proliferation, and differentiation by IGF1 secretion (Fontana et al., 2010; Parrella et al., 2013). Genetic reduction of insulin/IGF1 signaling was shown to elongate lifespan in lower-model organisms and female mice (Kenyon et al., 1993; Holzenberger et al., 2003; Bartke, 2005; Fontana et al., 2010). Insulin/IGF1 signaling is suppressed in response to DR, and this is believed to be one of the major mechanisms promoting improvements in health span in response to DR (Thissen et al., 1994; Fontana et al., 2010; Henning et al., 2013; Harvey et al., 2014). However, its role on hematopoiesis in the context of persistent DR has not been reported. We observed a decreased serum IGF1 level in DR-fed mice compared with AL-fed mice (Fig. 8 A). Of note, DR-mediated reductions in IGF1 levels were independent of p53 gene status (Fig. 8 B). To understand the role of IGF1 signaling on hematopoietic homeostasis under DR conditions, recombinant IGF1 protein or vehicle control was administered to DR-fed mice. IGF1 injection reverted the increase in quiescence of HSCs in DR-fed mice to almost the same level as in AL-fed mice (Fig. 8 C). However, this reversion in cell cycle did not rescue the impairment of lymphopoiesis but rather induced an even further enhancement of myelopoiesis/erythropoiesis in DR mice (Fig. 8, D–G). These results

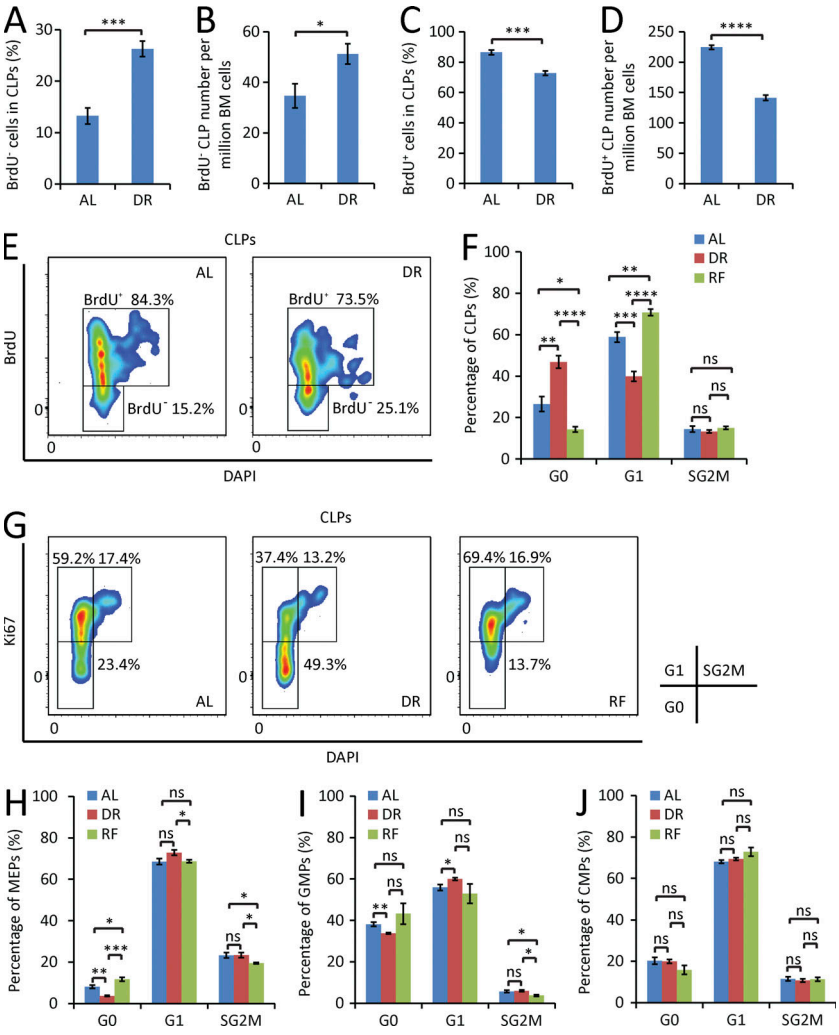

Figure 6. **DR selectively inhibits proliferation of lymphoid progenitors.** (A–E) Mice were treated with DR or AL for 6 d. On day 4, a single dose of 180 µg BrdU was injected intraperitoneally, and the mice were continuously supplied with 0.8 mg/ml BrdU in drinking water for the subsequent 2 d (n = 5 mice per group; n = 2 independent experiments). Percentage (A) and absolute number (B) of BrdU⁻ cells in the fraction of CLPs. Percentage (C) and absolute number (D) of BrdU⁺ cells in the fraction of CLPs. Unpaired two-tailed Student's t test was used. (E) Representative FACS plots gated from CLPs. (F–J) Cell cycle activity analysis of CLPs (F), MEPs (H), GMPs (I), and CMPs (J) in mice treated with DR or AL for 3 wk or refed for 3 d after 3 wk of DR (n = 4–5 mice per group; n = 2 independent experiments). One-way ANOVA analysis was used. (G) Representative FACS plots gated from CLPs. Data are displayed as mean ± SEM. *, P < 0.05; **, P < 0.01; ***, P < 0.001; ****, P < 0.0001. ns, not significant.

indicated that DR-induced suppression of IGF1 contributes to the increase in HSC quiescence but not to the impairment in lymphopoiesis in response to DR.

Suppression of IL-6/IL-7 contributes to the impairment of lymphopoiesis in response to DR

Several interleukins are known mediators of lymphopoiesis, such as IL-6 and IL-7. In particular, IL-7 is a nonredundant cytokine, which is essential for T and B cell development (Alpdogan et al., 2001; Mackall et al., 2011). It is important for proliferation, differentiation, and survival of B and T cell precursors (Akashi et al., 1998; Corcoran et al., 1998). IL-7– or IL-7Rα–deficient mice or anti–IL-7 antibody–treated mice all display severely impaired B- and T cell development (Peschon et al., 1994; von Freeden-Jeffry et al., 1995). Of note, serum levels of IL-7 were strongly reduced in response to DR, and this response was completely rescued by RF (Fig. 9 A). To test whether down-regulation of IL-7 contributed to the impaired B lymphopoiesis in DR-fed mice, DR-fed mice were treated with daily injections of IL-7 or vehicle controls. Intriguingly, IL-7 injection significantly reverted the DR-mediated reduction of CLPs (Fig. 9 B) and pro–B cells (not depicted), as well as the DR-mediated increases in the number of MEPs in BM (Fig. 9 C). This rescue in the skewing of hematopoiesis in DR-fed mice was associated with a reduction of quiescence of CLPs (Fig. 9 D) and an induction of proliferation of pro–B cells (not depicted) in response to IL-7 supplementation. Interestingly, IL-7 injection also rescued the cell differentiation of lymphoid-biased HSCs into CLPs and differentiation of CLPs into pro–B cells in DR-fed mice (Fig. 9, E and F), accompanied by a rescue in the skewed expression of genes that control lymphoid cell differentiation versus genes controlling erythroid cell differentiation in HSCs (Fig. 9 G).

IL-6 is another cytokine that plays an important role in hematopoiesis, including B cell development (Hirano et al., 1986; Patchen et al., 1991). In accordance with previous studies (Spaulding et al., 1997b; Chung et al., 2002; Ugochukwu and Figgers, 2007; You et al., 2007), we also ob-

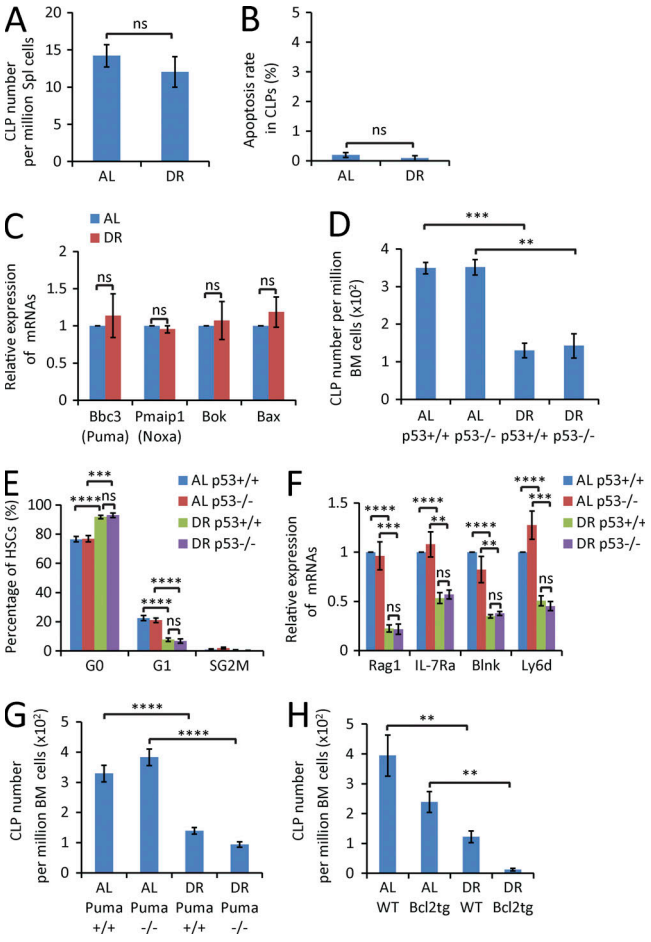

Figure 7. **Impairment of lymphopoiesis is not the result of CLP mobilization or apoptosis.** (A and B) FACS analysis of CLPs in spleen (Spl) of 2-mo-old mice treated for 2 wk with a DR or AL diet. (A) Absolute number of CLPs in BM (n = 4 mice per group; n = 2 independent experiments). (B) Percentage of apoptosis (Annexin V positive and DAPI negative) in the fraction of CLPs (n = 5 mice per group; n = 2 independent experiments). Unpaired two-tailed Student's t test was used. (C) qRT-PCR analysis of the mRNA expression of the indicated apoptosis-inducing genes in the fraction of freshly isolated CLPs from BM of 2-mo-old mice treated for 2 wk with a DR or AL diet (n = 4 independent experiments). For each experiment, CLPs were extracted from a pool of three mice per group, and expression levels were normalized to β-actin and set to 1 in CLPs derived from AL diet–treated mice. Unpaired two-tailed Student's t test was used. (D–F) 2-mo-old $p53^{-/-}$ mice and $p53^{+/+}$ mice (littermates) were treated with DR or AL for 2 wk (n = 3–4 mice per group; n = 2 independent experiments). (D) Total number of CLPs analyzed by FACS. (E) Cell cycle activity analysis of HSCs analyzed by Ki67 and DAPI staining. (F) qRT-PCR analysis of the expression of lymphoid-specific genes in lymphoid-biased HSCs. One-way ANOVA analysis was used. (G) FACS analysis of the total number of CLPs from 8-mo-old $Puma^{-/-}$ mice and $Puma^{+/+}$ mice (littermates) that were treated with a DR or AL diet for 2 wk (n = 3 mice per group; n = 2 independent experiments). One-way ANOVA analysis was used. (H) FACS analysis of total number of CLPs from 7-mo-old Bcl2 transgenic mice and age- and gender-matched WT mice that were treated with a DR or AL diet for 2 wk (n = 3–4 mice per group; n = 2 independent experiments). Data are displayed as mean ± SEM. *, $P < 0.05$; **, $P < 0.01$; ***, $P < 0.001$; ****, $P < 0.0001$ by one-way ANOVA. ns, not significant.

served a suppression of IL-6 expression in the serum of DR mice (Fig. 9 H). Similar to experiments on IL-7, injection of IL-6 rescued the production of CLPs in DR-fed mice (Fig. 9 I). These data indicated that the lowered expression of IL-7 and IL-6 contribute to the skewed differentiation of HSCs under DR condition.

It is known that DR elevates serum levels of corticosterone in rats and mice (Klebanov et al., 1995; Han et al., 2001; Harper et al., 2006), possibly resulting from a stress response triggered by DR. Because glucocorticoids suppress immune activity, we investigated the possible contribution of hypercorticism to the skewing in hematopoiesis/lymphopoiesis in response to DR. To this end, adrenalectomy (ADX) or sham operation was conducted. 10 d after the surgery, mice were treated with DR or AL. In line with previous studies (Han et al., 2001; Harper et al., 2006), serum levels of total corticosterone were significantly elevated in DR mice compared with the AL mice in the sham-operated group, whereas corticosterone levels were significantly reduced in the ADX group both in DR- and AL-fed mice (Fig. 9 J). ADX partially rescued the reduction of CLPs (Fig. 9 K) but not the inhibition of cell cycle activity of CLPs (Fig. 9 L) and pro–B cells (not depicted) or the increases in erythropoiesis in mice exposed to DR conditions (Fig. 9 M). Moreover, the DR-induced skewing in the expression of genes that control lymphoid cell differentiation versus genes controlling erythroid cell differentiation in HSCs was not rescued by ADX (Fig. 9 N). Also, the serum levels of IL-7 and IL-6 were not affected by ADX (Fig. 9, O and P). Together, these data indicate that DR-induced hypercorticism contributes to DR-induced alteration in hematopoiesis/lymphopoiesis. However, removal of corticoids by ADX could not revert DR-mediated suppression in lymphopoiesis to the same extent as the supplementation of IL-6 and IL-7 and had no effect on the induction of erythropoiesis in DR-exposed mice, which was instead fully reverted by IL-7 supplementation. It would be interesting for future studies to further delineate IL-6/IL-7–dependent processes, corticosteroid-dependent processes, and interactions between these processes in altering HSC differentiation in response to DR.

DISCUSSION

The current study provides the first experimental evidence that long-term application of 30% DR, the best-studied anti-aging intervention across different species, induces beneficial and adverse effects on HSC aging and hematopoiesis/lymphopoiesis. The study shows that despite having beneficial effects on retarding decline in the repopulation capacity of HSCs during aging, DR severely impairs lymphopoiesis by impairing the differentiation of lymphoid-biased HSCs and lymphoid progenitor cell proliferation. The study identifies specific systemic acting factors (e.g., decreases in IL-6, IL-7, and IGF1) that mediate beneficial and adverse effects of DR on HSC function and hematopoiesis.

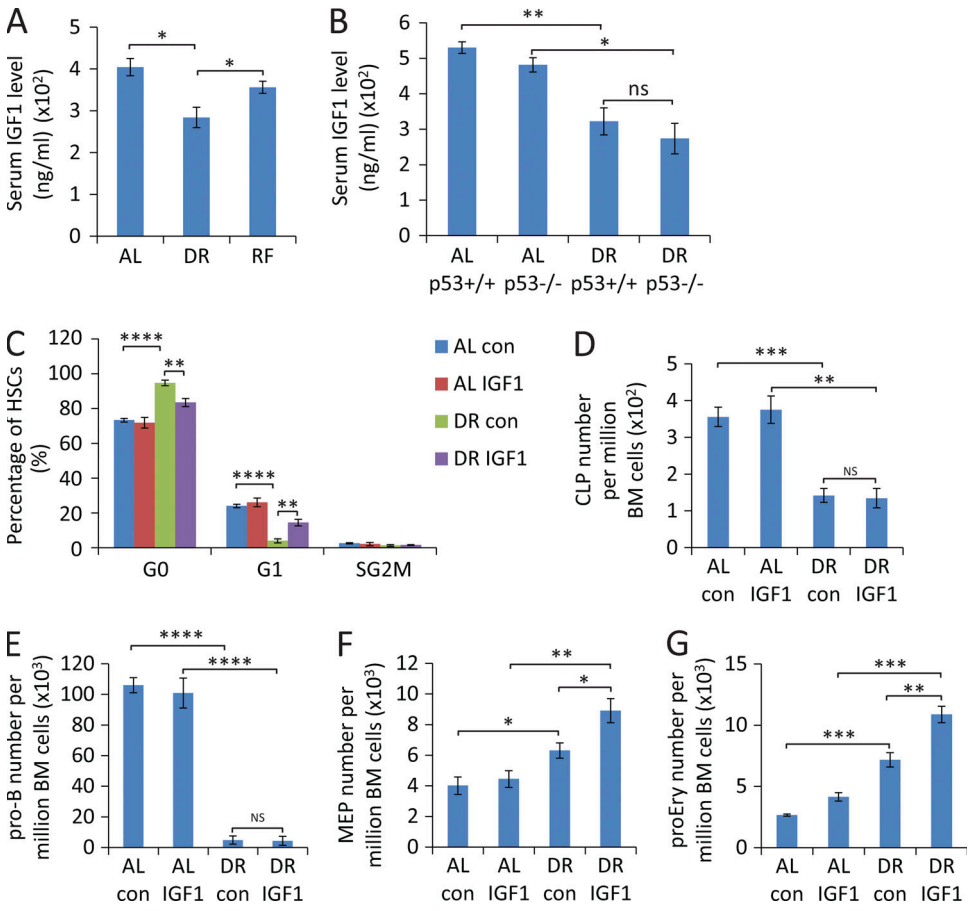

Figure 8. **IGF1 injection reverts the increases in HSC quiescence but not the suppression of lymphopoiesis in mice exposed to DR.** (A) ELISA-determined serum level of IGF1 in mice treated with DR or AL for 4 d or refed with an AL diet for 3 d after 4 d of DR (n = 3–4 mice per group; n = 2 independent experiments). (B) ELISA-determined serum level of IGF1 in 2-mo-old $p53^{-/-}$ mice and $p53^{+/+}$ mice (littermates) that were treated with DR or AL for 2 wk (n = 3–4 mice per group; n = 2 independent experiments). (C–G) Mice were treated with a DR or AL diet for 8 d. In parallel, recombinant human IGF1 protein or vehicle control was subcutaneously injected twice per day at a dose of 500 µg/kg (n = 4 mice per group; n = 2 independent experiments). FACS analysis was performed 24 h after the last injection on freshly isolated BM cells: percentage of HSCs in the indicated cell cycle stages (C), total numbers of CLPs (D), pro–B cells (E), MEPs (F), and proEry's (G) per million total BM cells are show. AL con, control-injected AL mice; AL IGF1, IGF1-injected AL mice; DR con, control-injected DR mice; DR IGF1, IGF1-injected DR mice. Data are displayed as mean ± SEM. *, P < 0.05; **, P < 0.01; ***, P < 0.001; ****, P < 0.0001 by one-way ANOVA. ns, not significant.

DR increases HSC quiescence and retards HSC aging

The long-term self-renewal capacity of adult HSCs is not unlimited, and quiescence is believed to be a major mechanism to maintain HSC homeostasis (Wilson et al., 2008). In agreement with this hypothesis, it was shown that increasing HSC cycling leads to exhaustion of stem cells in many genetically modified mouse models (Qian et al., 2007; Yoshihara et al., 2007; Thorén et al., 2008; Wilson et al., 2008). Moreover, replication stress was shown to exhaust the self-renewal and functionality of HSCs by replication-induced reactive oxygen species levels and DNA damage (Walter et al., 2015), a process that appears to be accelerated by increases in replication stress during aging (Flach et al., 2014).

Previous studies estimated the doubling time of individual HSCs to be 17.8–145 d (Bradford et al., 1997; Cheshier et al., 1999; Kiel et al., 2007; Wilson et al., 2008), although there exists a predominantly dormant subpopulation (<1,000 cells per mouse, dividing only five times during lifetime), which is unlikely to significantly contribute to daily maintenance of adult hematopoiesis as a result of their extremely rare production of progeny (Wilson et al., 2008; Sun et al., 2014; Busch et al., 2015).

This study revealed a previously unknown effect of DR to increase HSC quiescence. To date, DR is discussed as one of the viable interventions that could eventually be applied to mankind to increase health and lifespan (Cheng et al., 2014; Longo and Mattson, 2014). Decreasing the fraction of cycling HSCs by DR could contribute to its health-promoting effects by reducing the overall turnover of the HSC pool. In support of this hypothesis, our study showed that long-term

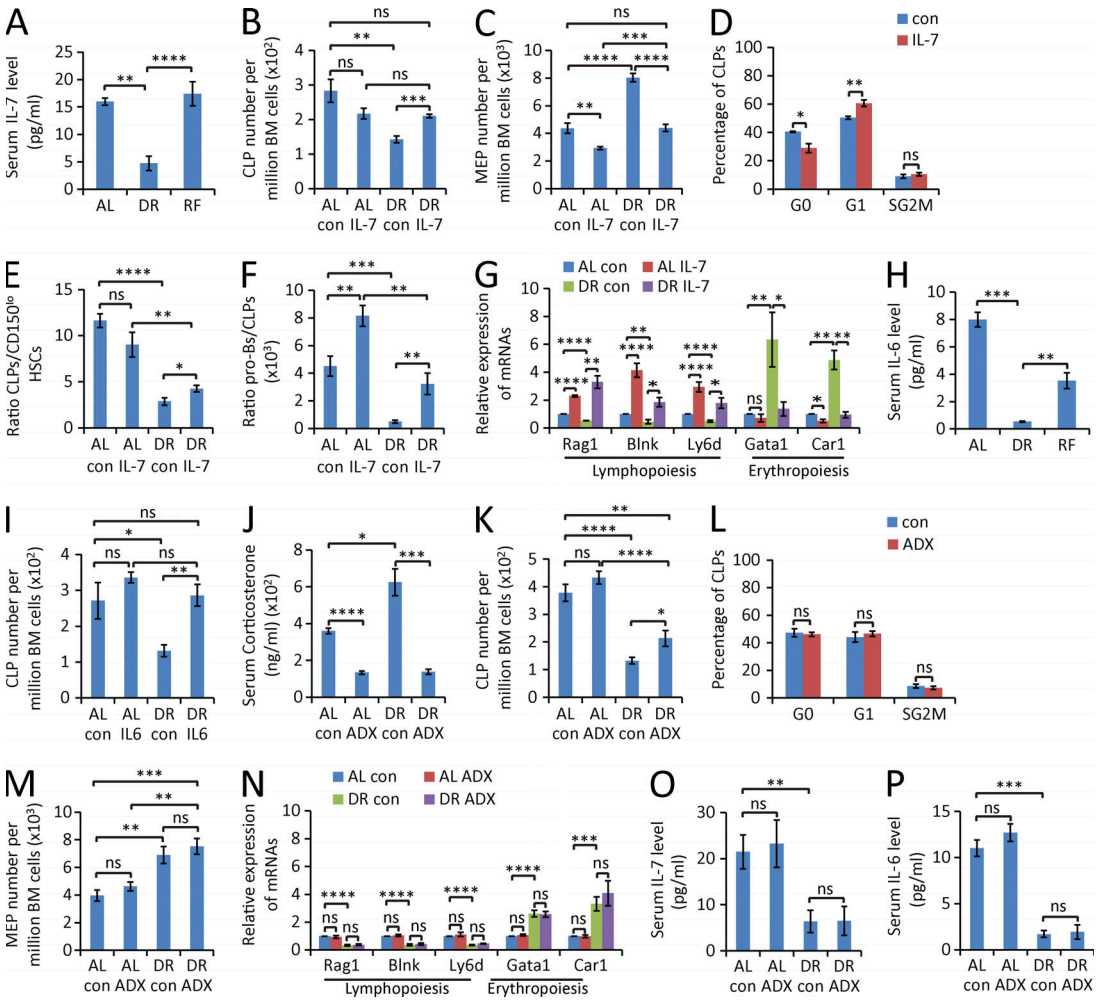

Figure 9. **IL-7 or IL-6 injection reverts suppression of lymphopoiesis in mice exposed to DR.** (A) ELISA-determined serum level of IL-7 in mice treated with DR or AL for 7 d or refed with AL diet for 3 d after 7 d of DR (n = 3–4 mice per group; n = 2 independent experiments). One-way ANOVA. (B–G) 2-mo-old mice were treated with DR or AL diet for 9 d. In parallel, mouse IL-7 protein or vehicle control was subcutaneously injected for 9 d at a dose of 50 µg/kg once per day (n = 5 mice per group; n = 2 independent experiments). Mice were sacrificed for analysis 24 h after the last injection. (B–D) FACS analysis was performed on freshly isolated BM cells to determine the total number of CLPs (B) and MEPs (C), and the percentage of CLPs (D) of DR mice in the indicated phases of the cell cycle (FACS analysis by Ki67 and DAPI staining). (E and F) the ratio of CLPs versus lymphoid-biased HSCs (E) and of pro–B cells versus CLPs (F). (G) The mRNA expression levels of genes that are associated with lymphoid cell differentiation and erythroid cell differentiation were determined by qRT-PCR in freshly isolated lymphoid-biased HSCs under the indicated treatment conditions. One-way ANOVA (B, C, and E–G) or unpaired two-tailed Student's t test (D) was used. (H) ELISA-determined serum level of IL-6 in mice treated with DR or AL for 7 d or refed with AL diet for 3 d after 7 d of DR (n = 3–4 mice per group; n = 2 independent experiments). One-way ANOVA was used. (I) 2-mo-old mice were treated with a DR or AL diet for 5 d. In parallel, mouse IL-6 protein or vehicle control was subcutaneously injected into mice daily at a dose of 50 µg/kg (n = 4 mice per group; n = 2 independent experiments). The total number of CLPs was determined by FACS analysis, 24 h after the last injection. One-way ANOVA analysis. (J–P) ADX or sham surgery was performed on 2-mo-old mice. 10 d after operation, mice were treated with DR or AL for 9 d (n = 4–5 mice per group; n = 2 independent experiments). Mice of the indicated cohorts were analyzed as follows: (J, O, and P) ELISA-determined serum levels of total corticosterone (J), IL-7 (O), and IL-6 (P); (K–M) FACS analysis of the total number of CLPs (K) and MEPs (M) per million BM cells and of the percentage of CLPs (L) of DR mice in different stages of the cell cycle (by Ki67 and DAPI staining); (N) expression of lymphoid- and erythroid-specific genes in lymphoid-biased HSCs of mice of the indicated cohorts. One-way ANOVA (J, K, and M–P) or unpaired two-tailed Student's t test (L) was used. AL con, control-injected AL mice or sham-operated AL mice; AL IL-7, IL-7–injected AL mice; DR con, control-injected DR mice or sham-operated DR mice; DR IL-7, IL-7–injected DR mice; AL IL-6, IL-6–injected AL mice; DR IL-6, IL-6–injected DR mice; AL ADX, AL mice with ADX; DR ADX, DR mice with ADX. Data are displayed as mean ± SEM. *, $P < 0.05$; **, $P < 0.01$; ***, $P < 0.001$; ****, $P < 0.0001$. ns, not significant.

DR prevented the induction of typical aging phenotypes of HSCs characterized by an increase in the pool size of phenotypically defined HSCs, skewing toward myeloid-biased HSCs versus lymphoid-biased HSCs, and impairments in the repopulation capacity of HSCs. Mechanistically, the improved maintenance of the repopulating activity of HSCs during

early aging by long-term DR may involve the DR-mediated reduction of oxidative stress–induced damage (López-Lluch et al., 2006; Qiu et al., 2010). HSCs in quiescence were shown to reside in a state of low metabolic activity characterized by glycolytic activity and low rates of oxidative phosphorylation–dependent glucose metabolism (Suda et al., 2005, 2011). In addition, HSC proliferation by itself was shown to induce reactive oxygen species levels that in turn aggravate DNA damage and HSC exhaustion in the context of DNA repair deficiencies (Walter et al., 2015). It is possible that DR-induced quiescence of HSCs contributes to the beneficial effects of DR, delaying the functional exhaustion of HSCs during aging by the suppression of both cell cycle activity and metabolic activity.

Aging is a lifelong process that lasts from adulthood until advanced age. This study reveals DR-dependent effects during early aging until midlife. However, the observed effects of long-term DR that occur until midlife (reduced increase in HSC number, reduced myeloid skewing, and improved repopulation capacity) resemble a rescue of changes in the hematopoietic system that also characterize advanced aging. It remains to be investigated whether DR would continue to affect these phenotypes until advanced age.

DR impairs lymphoid cell differentiation but induces erythroid/myeloid cell differentiation of HSCs and early progenitor cells

Despite the beneficial effect on HSC maintenance, this study shows that DR leads to a severe impairment of lymphopoiesis. Interestingly, there is a sequential suppression (in response to DR) and recovery (in response to RF) of B lymphopoiesis starting at the earliest lymphoid progenitor cell level (CLPs) and proceeding through intermediate stages toward mature B cells. This sequential alteration in B lymphopoiesis in response to DR is distinct from other stresses (such as irradiation) that suppress the lymphoid lineage, mainly involving apoptosis of downstream lymphocytes (Yin et al., 2000; Dainiak, 2002). In contrast, DR-induced suppression of lymphopoiesis is not associated with apoptosis induction but originates from a suppression of differentiation and proliferation starting at the tip of the hierarchy—the lymphoid-biased HSCs and early lymphoid progenitor cells (CLPs). This suppression of lymphopoiesis in response to DR coincides with a suppression of expression of key genes that regulate lymphoid fate determination as well as with impaired proliferation of early lymphoid progenitor cells.

In contrast to the suppression of B lymphopoiesis, erythropoiesis/myelopoiesis was enhanced upon DR. Long-term DR leads to an elevated expression of erythroid-specific genes in HSCs, and rates of erythroid/myeloid progenitor cell proliferation remain high in response to DR in contrast to the suppression of lymphoid progenitor cell proliferation. Previously, it was shown that hematopoietic progenitor cells (GMPs) undergo apoptosis upon extreme DR (fasting mice for 24 h; Warr et al., 2013), and repeated fasting (fasting mice for 48 h) and RF cycles were found to reverse age-dependent myeloid bias (Cheng et al., 2014). However, as shown in this study, moderate long-term DR does not result in myeloid progenitor cell apoptosis but strongly impairs B lymphopoiesis by impairing HSC differentiation and progenitor cell proliferation. Together, these results show that constant and moderate DR has a very different impact on HSCs and progenitor cells compared with cycles of extreme DR (fasting) and RF.

Down-regulation of growth factors such as IGF1 is generally considered as one of the key mechanisms of DR-mediated effects in other model systems. This study shows that IGF1 suppression contributes to DR-induced HSC quiescence but does not regulate the impairment of B lymphopoiesis, which is rather related to the suppression of IL-7 and IL-6 in response to DR. Of note, IL-7 injection rescued not only the DR-induced inhibition of proliferation of lymphoid progenitors and the lymphoid cell differentiation block of HSCs, but it also reduced the enhancement of erythropoiesis and therefore reverted the skewing in hematopoiesis under long-term DR. IL-7 and IL-6 are produced by various types of cells from multiple organs including thymus, muscle, skin, intestine, and adipose tissue (Mackall et al., 2011; Hara et al., 2012; Mihara et al., 2012), many of which are known to be affected by calorie restriction (Loewenthal and Montagna, 1955; Mittal et al., 1988; Lyra et al., 1993; Devlin et al., 2010; Clevers, 2012; Yilmaz et al., 2012). The reduced levels of IL-6/IL-7 under DR conditions are likely the result of systemic changes in multiple organs and appear to contribute to the saving of energy expenditure in dietary restricted situation.

Collectively, the current study provides experimental evidence for a dual role of DR in maintaining HSC repopulation capacity during aging but skewing the capacity of HSCs and early progenitor cells to maintain balanced differentiation toward lymphopoiesis and erythropoiesis/myelopoiesis. Historically, there have been observations of low blood lymphocytes and increased RBCs in mammals under DR (Hishinuma and Kimura, 1990; Walford et al., 2002; Ritz and Gardner, 2006). To our knowledge, this study provides the first mechanistic understanding of immune-suppressive effects of DR, which are regulated by a reduction of specific cytokines, resulting in altered expression of fate determination genes and impaired proliferation of lymphoid (biased) stem and progenitor cells. HSCs stand at the tip of the hierarchy of the hematopoietic system and, as such, are the main cell type to adjust hematopoiesis to different challenges, including the here-disclosed response to mild metabolic stress induced by DR, resulting in suppression of B lymphopoiesis and enhanced erythropoiesis. This adjustment of HSCs could evolutionarily be important for the body to adapt to energy stress in times of low food availability because RBCs are the transporters of oxygen, which is a fundamental component of the respiratory chain to efficiently produce energy. However, the suppression of lymphopoiesis and immune functions might also represent a relevant side effect contributing to the failure of long-term DR to elongate the lifespan in

long-lived mammals despite improving health parameters (Mattison et al., 2012).

MATERIALS AND METHODS

Mice and dietary intervention. C57BL/6J mice were obtained from Janvier. p53 knockout mice, Puma knockout mice, and Vav-Bcl2 transgenic mice were maintained on a C57BL/6J background (Donehower et al., 1992; Ogilvy et al., 1999; Jeffers et al., 2003). Mice were maintained in the animal facilities of the Leibniz Institute on Aging on a 12-h light/12-h dark cycle. Mice were housed individually and received a regimen of either an AL diet (fed with an unlimited amount of food) or a DR diet (fed daily with an amount of food corresponding to 70% of the amount of food consumed by body weight– and gender-matched mice in the AL group). The provided food amount was constant over the whole DR period. All mouse experiments were approved by the state government of Thüringen (protocol number 03-006/13).

BrdU administration. BrdU (Sigma-Aldrich) was administered by 180 µg/mouse intraperitoneal injection as a single dose followed by supplying drinking water at a concentration of 0.8 mg/ml.

pIpC administration. pIpC (Sigma-Aldrich) was administered by 5-mg/kg intraperitoneal injection as a single dose.

Flow cytometry. Mice were sacrificed, and BM was flushed from all hind limbs and pelvis with sterile PBS. BM cells were resuspended in a 150-mM ammonium chloride solution to lyse the red cells. Afterward, cells were washed, counted, and incubated with flow cytometric antibodies. Phenotypic cell surface markers for HSCs, CMPs, GMPs, and MEPs were detected using a lineage cocktail (biotinylated anti-B220, -CD11b, –Gr-1, –TER-119, -CD3, -CD4, and -CD8 antibodies; BioLegend) and Alexa Fluor 700–conjugated anti-CD34 (eBioscience), APC-conjugated anti-CD150 (BioLegend), PE-Cy7–conjugated anti–c-Kit (eBioscience), Pacific blue–conjugated anti–Sca-1 (BioLegend), FITC-conjugated anti-CD16/32 (BioLegend) antibodies, and streptavidin-APC-Cy7 (BioLegend). Phenotypic cell surface markers for CLPs were detected using a lineage cocktail (biotinylated anti-B220, -CD11b, –Gr-1, –TER-119, -CD3, -CD4, and -CD8 antibodies) and PerCP-Cy5.5–conjugated anti–IL-7Rα (eBioscience), PE-conjugated anti-Flt3 (BioLegend), APC-conjugated anti–c-Kit (BioLegend), PE-Cy7–conjugated anti–Sca-1 (BioLegend) antibodies, and streptavidin-APC-Cy7. Phenotypic cell-surface markers for pro–B cells were detected using a lineage cocktail (biotinylated anti–Gr-1, -CD11b, –TER-119, and -CD3 antibodies) and APC-Cy7–conjugated anti-CD19 (BioLegend), Pacific blue–conjugated anti-B220 (BioLegend), PE-conjugated anti-CD43 (BD), APC-conjugated anti-AA4.1 (eBioscience), FITC-conjugated anti-CD24 (BioLegend) antibodies, and streptavidin–Alexa Fluor 700. Phenotypic cell surface markers for proEry's were detected using APC-conjugated anti–TER-119 (eBioscience) and PE-conjugated anti-CD71 (BioLegend) antibodies. Phenotypic cell surface markers for differentiated BM cells were detected using PE-conjugated anti-B220 (BioLegend), APC-Cy7–conjugated anti-CD11b (BioLegend), FITC-conjugated anti–Gr-1 (eBioscience), APC-conjugated anti-CD4 (BioLegend), and PerCP-Cy5.5–conjugated anti-CD8 (BioLegend) antibodies. After staining, cells were analyzed on a flow cytometer (FACS LSR Fortessa; BD).

For cell cycle analysis, BM cells were first stained with certain antibody combinations to label populations of interest. For HSCs, a lineage cocktail as described in the previous paragraph and Alexa Fluor 700–conjugated anti-CD34, PE-conjugated anti-CD150 (BioLegend), APC-conjugated anti–c-Kit, PE-Cy7–conjugated anti–Sca-1 (BioLegend), and PerCP-Cy5.5–conjugated anti-CD48 antibodies and streptavidin–APC-Cy7 were used. For CLPs, a lineage cocktail as described in the previous paragraph and PerCP-Cy5.5–conjugated anti–IL-7Rα, PE-conjugated anti-Flt3, APC-conjugated anti–c-Kit, PE-Cy7–conjugated anti-Sca-1 antibodies, and streptavidin-APC-Cy7 were used. For CMPs/GMPs/MEPs, a lineage cocktail as described above and PE-Cy7–conjugated anti-CD16/32, Alexa Fluor 700–conjugated anti-CD34, APC-conjugated anti–c-Kit, PE-conjugated anti–Sca-1 antibodies, and streptavidin-APC-Cy7 were used. For pro–B cells, a lineage cocktail (biotinylated anti–Gr-1, -CD11b, –TER-119, and -CD3 antibodies) and APC-Cy7–conjugated anti-CD19, Pacific blue–conjugated anti-B220, APC-conjugated anti-AA4.1, PE-conjugated anti-CD24 (BioLegend) antibodies, and streptavidin–Alexa Fluor 700 were used. After staining, cells were fixed and permeabilized with the Cytofix/Cytoperm Fixation/Permeabilization Solution kit (BD) according to the manufacturer's instructions. Afterward, cells were incubated with FITC-conjugated anti-Ki67 antibody (BD) for 1 h on ice and incubated with DAPI/PBS medium to stain for DNA contents. BrdU staining was performed using the BrdU Flow kit (BD) according to the manufacturer's instructions.

HSC sorting. BM cells were incubated with APC-conjugated anti–c-Kit antibody, and c-Kit$^+$ cells were enriched using anti-APC magnetic beads and LS columns (Miltenyi Biotec). The positively selected cells were then stained for HSC markers using a lineage cocktail as described in the previous section and Alexa Fluor 700–conjugated anti-CD34, Brilliant Violet 605–conjugated anti-CD150 (BioLegend), PE-Cy7–conjugated anti-CD48 (BioLegend), APC-conjugated anti–c-Kit, and PE-conjugated anti–Sca-1 (BioLegend) antibodies and streptavidin-APC-Cy7. After staining, cells were sorted on a cell sorter (FACSAria III; BD).

BM transplantation. 100 or 200 FACS-purified HSCs from Ly5.2 donor mice mixed with 2×10^5 BM cells from Ly5.1 mice were injected via tail vein into lethally irradiated Ly5.1/5.2 recipient mice. 4 mo after primary transplantation, 10^7 BM cells from the primary recipients were transplanted

into secondary recipient mice (Ly5.1/5.2). BM analysis was performed 4 mo after transplantation.

PB cell counting. PB was collected from the tail vein containing a minimal volume of 0.5 M EDTA. PB cell count was performed on cell counter (model 2000; AL Systeme) according to the manufacturer's instructions.

***Staphylococcus aureus* infection.** Mice were inoculated subcutaneously with 2×10^7 CFU of *S. aureus* 6850 bacteria by injecting 50 µl of the cell suspension (4×10^8 cells/ml in PBS) into the left hind footpad. Six mice per group (AL and DR) were infected. Mice were sacrificed by CO_2 asphyxiation 1 wk after infection, and CFU counts of footpads were determined. Colonies were counted after incubation of homogenized tissue overnight at 37°C.

RNA isolation and cDNA synthesis. Total RNA was isolated from freshly sorted cells by using MagMAX-96 Total RNA Isolation kit (Ambion). A DNA digestion step was included during the RNA purification process. Reverse transcriptions were performed to synthesize first-strand DNA by using the GoScript reverse transcription system (Promega).

Quantitative real-time PCR (qRT-PCR). qRT-PCR was performed with an ABI 7500 Real-Time PCR System (Applied Biosystems). iTaq SYBR green supermix with Rox (Bio-Rad Laboratories) was used. mRNA expression of genes was normalized to β-actin in each sample and was normalized to 1 in the AL group. Primer sets for the detection of single genes are listed as follows. β-actin–F, 5′-CTAAGGCCA ACCGTGAAAAG-3′; β-actin–R, 5′-ACCAGAGGCATA CAGGGACA-3′; Rag1-F, 5′-TCCCAGCACACTTTG TGAAA-3′; Rag1-R, 5′-GGGATCAGCCAGAATGTG TT-3′; IL-7Rα–F, 5′-CGAAACTCCAGAACCCAAGA-3′; IL-7Rα–R, 5′-AATGGTGACACTTGGCAAGAC-3′; Blnk-F, 5′-TCCCATTTAATTCGACGTTTG-3′; Blnk-R, 5′-AGCATACCAGGGCTTACCG-3′; Ly6d-F, 5′-TCT GCTCGTCCTCCTTGTCT-3′; Ly6d-R, 5′-GTGCAC ACGTGACATCGAA-3′; CEBPα-F, 5′-AAACAACGC AACGTGGAGA-3′; CEBPα-R, 5′-GCGGTCATTGTC ACTGGTC-3′; Mpo-F, 5′-TCGATGGAATGGGGAGAA-3′; Mpo-R, 5′-TCCCGGTATGTGATGATCTG-3′; Gata1-F, 5′-GAGCTGACTTTCCCAGTCCTT-3′; Gata1-R, 5′-CACACACTCTCTGGCCTCAC-3′; Car1-F, 5′-CAG AAAGTACTTGATGCTCTAAACTCA-3′; Car1-R, 5′-AAGTAGGTCCAGTAATCCAGAGATG-3′; Bbc3-F, 5′-TGGAGGGTCATGTACAATCTCTT-3′; Bbc3-R, 5′-GTTGGGCTCCATTTCTGG-3′; Pmaip1-F, 5′-CAGATG CCTGGGAAGTCG-3′; Pmaip1-R, 5′-TGAGCACAC TCGTCCTTCAA-3′; Bok-F, 5′-AGTGGCAGGCCACAT CTT-3′; Bok-R, 5′-CCACGGAATACAGGGACACTA-3′; Bax-F, 5′-GTGAGCGGCTGCTTGTCT-3′; Bax-R, 5′-GGTCCCGAAGTAGGAGAGGA-3′.

ELISA. ELISA for detecting IGF1, IL-6, IL-7, and total corticosterone was performed using the IGF-I mouse/rat ELISA kit (Mediagnost), the Mouse IL-6 Quantikine ELISA kit (R&D Systems), the Mouse IL-7 Quantikine ELISA kit (R&D Systems), and Corticosterone EIA kit (ARBOR ASSAYS), respectively, according to the manufacturer's instructions.

Administration of IGF1, IL-7, and IL-6. Recombinant human IGF1 (Mecasermin [Increlex; Tatzend Apotheke]) was subcutaneously injected into mice twice per day for 8 d at a dose of 500 µg/kg. Recombinant murine IL-7 protein (antibodies online Inc.) was subcutaneously injected into mice daily for 9 d at a dose of 50 µg/kg. Recombinant murine IL-6 protein (PeproTech) was subcutaneously injected into mice daily for 5 d at a dose of 50 µg/kg.

ADX. Mice were anesthetized with 95 mg/kg ketamine and 8 mg/kg xylazin, and adrenal glands from both sides were removed. Sham operation was performed with the same surgical steps without removing the adrenal glands. 1% NaCl was provided in drinking water throughout the experimental period after the surgery to both operation and sham operation groups.

Statistics. Prism 6.0 software (GraphPad Software) was used for all statistical analysis. The unpaired two-tailed Student's *t* test and one-way ANOVA was used to calculate p-values for two-group datasets and multigroup (more than two groups) datasets, respectively.

Online supplemental material. Fig. S1 shows the FACS gating strategy of HSCs and myeloid/erythroid progenitors in flow cytometry analysis. Fig. S2 shows the FACS gating strategy of CLPs in flow cytometry analysis. Fig. S3 shows the FACS gating strategy of pro–B cells in flow cytometry analysis. Fig. S4 shows the FACS gating strategy of B cells, myeloid cells, and proEry's in flow cytometry analysis. Online supplemental material is available at http://www.jem.org/cgi/content/full/jem.20151100/DC1.

ACKNOWLEDGEMENTS

This work was supported by the Deutsche Forschungsgemeinschaft (Ru745-10, RU-745-12), the European Union (ERC-2012-AdG 323136), the Federal Ministry of Education and Research (GerontoSys-SyStaR 315894), the state of Thuringia, and intramural funds from the Leibniz Association.

The authors declare no competing financial interests.

Submitted: 4 July 2015

Accepted: 26 January 2016

REFERENCES

Akashi, K., M. Kondo, and I.L. Weissman. 1998. Role of interleukin-7 in T-cell development from hematopoietic stem cells. *Immunol. Rev.* 165:13–28. http://dx.doi.org/10.1111/j.1600-065X.1998.tb01226.x

Alpdogan, O., C. Schmaltz, S.J. Muriglan, B.J. Kappel, M.A. Perales, J.A. Rotolo, J.A. Halm, B.E. Rich, and M.R. van den Brink. 2001. Administration

of interleukin-7 after allogeneic bone marrow transplantation improves immune reconstitution without aggravating graft-versus-host disease. *Blood*. 98:2256–2265. http://dx.doi.org/10.1182/blood.V98.7.2256

Bartke, A. 2005. Minireview: role of the growth hormone/insulin-like growth factor system in mammalian aging. *Endocrinology.* 146:3718–3723. http://dx.doi.org/10.1210/en.2005-0411

Beerman, I., D. Bhattacharya, S. Zandi, M. Sigvardsson, I.L. Weissman, D. Bryder, and D.J. Rossi. 2010. Functionally distinct hematopoietic stem cells modulate hematopoietic lineage potential during aging by a mechanism of clonal expansion. *Proc. Natl. Acad. Sci. USA*. 107:5465–5470. http://dx.doi.org/10.1073/pnas.1000834107

Beerman, I., C. Bock, B.S. Garrison, Z.D. Smith, H. Gu, A. Meissner, and D.J. Rossi. 2013. Proliferation-dependent alterations of the DNA methylation landscape underlie hematopoietic stem cell aging. *Cell Stem Cell*. 12:413–425. http://dx.doi.org/10.1016/j.stem.2013.01.017

Bradford, G.B., B. Williams, R. Rossi, and I. Bertoncello. 1997. Quiescence, cycling, and turnover in the primitive hematopoietic stem cell compartment. *Exp. Hematol.* 25:445–453.

Busch, K., K. Klapproth, M. Barile, M. Flossdorf, T. Holland-Letz, S.M. Schlenner, M. Reth, T. Höfer, and H.R. Rodewald. 2015. Fundamental properties of unperturbed haematopoiesis from stem cells in vivo. *Nature.* 518:542–546. http://dx.doi.org/10.1038/nature14242

Cerletti, M., Y.C. Jang, L.W. Finley, M.C. Haigis, and A.J. Wagers. 2012. Short-term calorie restriction enhances skeletal muscle stem cell function. *Cell Stem Cell*. 10:515–519. http://dx.doi.org/10.1016/j.stem.2012.04.002

Chambers, S.M., and M.A. Goodell. 2007. Hematopoietic stem cell aging: wrinkles in stem cell potential. *Stem Cell Rev.* 3:201–211. http://dx.doi.org/10.1007/s12015-007-0027-1

Chen, J., C.M. Astle, and D.E. Harrison. 1998. Delayed immune aging in diet-restricted B6CBAT6 F1 mice is associated with preservation of naive T cells. *J. Gerontol. A Biol. Sci. Med. Sci.* 53A:B330–B337. http://dx.doi.org/10.1093/gerona/53A.5.B330

Chen, J., C.M. Astle, and D.E. Harrison. 1999. Development and aging of primitive hematopoietic stem cells in BALB/cBy mice. *Exp. Hematol.* 27:928–935. http://dx.doi.org/10.1016/S0301-472X(99)00018-1

Chen, J., C.M. Astle, and D.E. Harrison. 2003. Hematopoietic senescence is postponed and hematopoietic stem cell function is enhanced by dietary restriction. *Exp. Hematol.* 31:1097–1103. http://dx.doi.org/10.1016/S0301-472X(03)00238-8

Cheng, C.W., G.B. Adams, L. Perin, M. Wei, X. Zhou, B.S. Lam, S. Da Sacco, M. Mirisola, D.I. Quinn, T.B. Dorff, et al. 2014. Prolonged fasting reduces IGF-1/PKA to promote hematopoietic-stem-cell-based regeneration and reverse immunosuppression. *Cell Stem Cell*. 14:810–823. http://dx.doi.org/10.1016/j.stem.2014.04.014

Cheng, T., H. Shen, D. Giokas, J. Gere, D.G. Tenen, and D.T. Scadden. 1996. Temporal mapping of gene expression levels during the differentiation of individual primary hematopoietic cells. *Proc. Natl. Acad. Sci. USA*. 93:13158–13163. http://dx.doi.org/10.1073/pnas.93.23.13158

Cheng, T., N. Rodrigues, H. Shen, Y. Yang, D. Dombkowski, M. Sykes, and D.T. Scadden. 2000. Hematopoietic stem cell quiescence maintained by p21cip1/waf1. *Science.* 287:1804–1808. http://dx.doi.org/10.1126/science.287.5459.1804

Cheshier, S.H., S.J. Morrison, X. Liao, and I.L. Weissman. 1999. In vivo proliferation and cell cycle kinetics of long-term self-renewing hematopoietic stem cells. *Proc. Natl. Acad. Sci. USA*. 96:3120–3125. http://dx.doi.org/10.1073/pnas.96.6.3120

Chung, H.Y., H.J. Kim, K.W. Kim, J.S. Choi, and B.P. Yu. 2002. Molecular inflammation hypothesis of aging based on the anti-aging mechanism of calorie restriction. *Microsc. Res. Tech.* 59:264–272. http://dx.doi.org/10.1002/jemt.10203

Clevers, H. 2012. The Paneth cell, caloric restriction, and intestinal integrity. *N. Engl. J. Med.* 367:1560–1561. http://dx.doi.org/10.1056/NEJMcibr1208353

Cohen, E., J.F. Paulsson, P. Blinder, T. Burstyn-Cohen, D. Du, G. Estepa, A. Adame, H.M. Pham, M. Holzenberger, J.W. Kelly, et al. 2009. Reduced IGF-1 signaling delays age-associated proteotoxicity in mice. *Cell*. 139:1157–1169. http://dx.doi.org/10.1016/j.cell.2009.11.014

Colman, R.J., R.M. Anderson, S.C. Johnson, E.K. Kastman, K.J. Kosmatka, T.M. Beasley, D.B. Allison, C. Cruzen, H.A. Simmons, J.W. Kemnitz, and R. Weindruch. 2009. Caloric restriction delays disease onset and mortality in rhesus monkeys. *Science.* 325:201–204. http://dx.doi.org/10.1126/science.1173635

Corcoran, A.E., A. Riddell, D. Krooshoop, and A.R. Venkitaraman. 1998. Impaired immunoglobulin gene rearrangement in mice lacking the IL-7 receptor. *Nature.* 391:904–907. http://dx.doi.org/10.1038/36122

Dainiak, N. 2002. Hematologic consequences of exposure to ionizing radiation. *Exp. Hematol.* 30:513–528. http://dx.doi.org/10.1016/S0301-472X(02)00802-0

de Haan, G., W. Nijhof, and G. Van Zant. 1997. Mouse strain-dependent changes in frequency and proliferation of hematopoietic stem cells during aging: correlation between lifespan and cycling activity. *Blood*. 89:1543–1550.

Devlin, M.J., A.M. Cloutier, N.A. Thomas, D.A. Panus, S. Lotinun, I. Pinz, R. Baron, C.J. Rosen, and M.L. Bouxsein. 2010. Caloric restriction leads to high marrow adiposity and low bone mass in growing mice. *J. Bone Miner. Res.* 25:2078–2088. http://dx.doi.org/10.1002/jbmr.82

Donehower, L.A., M. Harvey, B.L. Slagle, M.J. McArthur, C.A. Montgomery Jr., J.S. Butel, and A. Bradley. 1992. Mice deficient for p53 are developmentally normal but susceptible to spontaneous tumours. *Nature.* 356:215–221. http://dx.doi.org/10.1038/356215a0

Dorshkind, K., E. Montecino-Rodriguez, and R.A. Signer. 2009. The ageing immune system: is it ever too old to become young again? *Nat. Rev. Immunol.* 9:57–62. http://dx.doi.org/10.1038/nri2471

El-Deiry, W.S., T. Tokino, V.E. Velculescu, D.B. Levy, R. Parsons, J.M. Trent, D. Lin, W.E. Mercer, K.W. Kinzler, and B. Vogelstein. 1993. *WAF1*, a potential mediator of p53 tumor suppression. *Cell*. 75:817–825. http://dx.doi.org/10.1016/0092-8674(93)90500-P

Ertl, R.P., J. Chen, C.M. Astle, T.M. Duffy, and D.E. Harrison. 2008. Effects of dietary restriction on hematopoietic stem-cell aging are genetically regulated. *Blood*. 111:1709–1716. http://dx.doi.org/10.1182/blood-2007-01-069807

Essers, M.A., S. Offner, W.E. Blanco-Bose, Z. Waibler, U. Kalinke, M.A. Duchosal, and A. Trumpp. 2009. IFNalpha activates dormant haematopoietic stem cells in vivo. *Nature.* 458:904–908. http://dx.doi.org/10.1038/nature07815

Flach, J., S.T. Bakker, M. Mohrin, P.C. Conroy, E.M. Pietras, D. Reynaud, S. Alvarez, M.E. Diolaiti, F. Ugarte, E.C. Forsberg, et al. 2014. Replication stress is a potent driver of functional decline in ageing haematopoietic stem cells. *Nature.* 512:198–202. http://dx.doi.org/10.1038/nature13619

Florian, M.C., K. Dörr, A. Niebel, D. Daria, H. Schrezenmeier, M. Rojewski, M.D. Filippi, A. Hasenberg, M. Gunzer, K. Scharffetter-Kochanek, et al. 2012. Cdc42 activity regulates hematopoietic stem cell aging and rejuvenation. *Cell Stem Cell*. 10:520–530. http://dx.doi.org/10.1016/j.stem.2012.04.007

Fontana, L., L. Partridge, and V.D. Longo. 2010. Extending healthy life span—from yeast to humans. *Science.* 328:321–326. http://dx.doi.org/10.1126/science.1172539

Gardner, E.M. 2005. Caloric restriction decreases survival of aged mice in response to primary influenza infection. *J. Gerontol. A Biol. Sci. Med. Sci.* 60:688–694. http://dx.doi.org/10.1093/gerona/60.6.688

Geiger, H., G. de Haan, and M.C. Florian. 2013. The ageing haematopoietic stem cell compartment. *Nat. Rev. Immunol.* 13:376–389. http://dx.doi.org/10.1038/nri3433

Goldberg, E.L., M.J. Romero-Aleshire, K.R. Renkema, M.S. Ventevogel, W.M. Chew, J.L. Uhrlaub, M.J. Smithey, K.H. Limesand, G.D. Sempowski, H.L. Brooks, and J. Nikolich-Žugich. 2015. Lifespan-extending caloric restriction or mTOR inhibition impair adaptive immunity of old mice by distinct mechanisms. *Aging Cell.* 14:130–138. http://dx.doi.org/10.1111/acel.12280

Han, E.S., T.R. Evans, J.H. Shu, S. Lee, and J.F. Nelson. 2001. Food restriction enhances endogenous and corticotropin-induced plasma elevations of free but not total corticosterone throughout life in rats. *J. Gerontol. A Biol. Sci. Med. Sci.* 56:B391–B397. http://dx.doi.org/10.1093/gerona/56.9.B391

Hara, T., S. Shitara, K. Imai, H. Miyachi, S. Kitano, H. Yao, S. Tani-ichi, and K. Ikuta. 2012. Identification of IL-7-producing cells in primary and secondary lymphoid organs using IL-7-GFP knock-in mice. *J. Immunol.* 189:1577–1584. http://dx.doi.org/10.4049/jimmunol.1200586

Harper, J.M., C.W. Leathers, and S.N. Austad. 2006. Does caloric restriction extend life in wild mice? *Aging Cell.* 5:441–449. http://dx.doi.org/10.1111/j.1474-9726.2006.00236.x

Harvey, A.E., L.M. Lashinger, D. Hays, L.M. Harrison, K. Lewis, S.M. Fischer, and S.D. Hursting. 2014. Calorie restriction decreases murine and human pancreatic tumor cell growth, nuclear factor-κB activation, and inflammation-related gene expression in an insulin-like growth factor-1-dependent manner. *PLoS One.* 9:e94151. http://dx.doi.org/10.1371/journal.pone.0094151

Henning, P.C., D.E. Scofield, K.R. Rarick, J.R. Pierce, J.S. Staab, H.R. Lieberman, and B.C. Nindl. 2013. Effects of acute caloric restriction compared to caloric balance on the temporal response of the IGF-I system. *Metabolism.* 62:179–187. http://dx.doi.org/10.1016/j.metabol.2012.07.004

Hirano, T., K. Yasukawa, H. Harada, T. Taga, Y. Watanabe, T. Matsuda, S. Kashiwamura, K. Nakajima, K. Koyama, A. Iwamatsu, et al. 1986. Complementary DNA for a novel human interleukin (BSF-2) that induces B lymphocytes to produce immunoglobulin. *Nature.* 324:73–76. http://dx.doi.org/10.1038/324073a0

Hishinuma, K., and S. Kimura. 1990. Dietary restriction augments erythropoiesis in mice. *Int. J. Vitam. Nutr. Res.* 60:379–382.

Hock, H., M.J. Hamblen, H.M. Rooke, J.W. Schindler, S. Saleque, Y. Fujiwara, and S.H. Orkin. 2004. Gfi-1 restricts proliferation and preserves functional integrity of haematopoietic stem cells. *Nature.* 431:1002–1007. http://dx.doi.org/10.1038/nature02994

Holzenberger, M., J. Dupont, B. Ducos, P. Leneuve, A. Géloën, P.C. Even, P. Cervera, and Y. Le Bouc. 2003. IGF-1 receptor regulates lifespan and resistance to oxidative stress in mice. *Nature.* 421:182–187. http://dx.doi.org/10.1038/nature01298

Jeffers, J.R., E. Parganas, Y. Lee, C. Yang, J. Wang, J. Brennan, K.H. MacLean, J. Han, T. Chittenden, J.N. Ihle, et al. 2003. Puma is an essential mediator of p53-dependent and -independent apoptotic pathways. *Cancer Cell.* 4:321–328. http://dx.doi.org/10.1016/S1535-6108(03)00244-7

Jones, D.L., and T.A. Rando. 2011. Emerging models and paradigms for stem cell ageing. *Nat. Cell Biol.* 13:506–512. http://dx.doi.org/10.1038/ncb0511-506

Ju, Z., H. Jiang, M. Jaworski, C. Rathinam, A. Gompf, C. Klein, A. Trumpp, and K.L. Rudolph. 2007. Telomere dysfunction induces environmental alterations limiting hematopoietic stem cell function and engraftment. *Nat. Med.* 13:742–747. http://dx.doi.org/10.1038/nm1578

Kastan, M.B., A.I. Radin, S.J. Kuerbitz, O. Onyekwere, C.A. Wolkow, C.I. Civin, K.D. Stone, T. Woo, Y. Ravindranath, and R.W. Craig. 1991. Levels of p53 protein increase with maturation in human hematopoietic cells. *Cancer Res.* 51:4279–4286.

Kenyon, C., J. Chang, E. Gensch, A. Rudner, and R. Tabtiang. 1993. A *C. elegans* mutant that lives twice as long as wild type. *Nature.* 366:461–464. http://dx.doi.org/10.1038/366461a0

Kiel, M.J., S. He, R. Ashkenazi, S.N. Gentry, M. Teta, J.A. Kushner, T.L. Jackson, and S.J. Morrison. 2007. Haematopoietic stem cells do not asymmetrically segregate chromosomes or retain BrdU. *Nature.* 449:238–242. http://dx.doi.org/10.1038/nature06115

Klebanov, S., S. Diais, W.B. Stavinoha, Y. Suh, and J.F. Nelson. 1995. Hyperadrenocorticism, attenuated inflammation, and the life-prolonging action of food restriction in mice. *J. Gerontol. A Biol. Sci. Med. Sci.* 50A:B78–B82. http://dx.doi.org/10.1093/gerona/50A.2.B78

Kondo, M., I.L. Weissman, and K. Akashi. 1997. Identification of clonogenic common lymphoid progenitors in mouse bone marrow. *Cell.* 91:661–672. http://dx.doi.org/10.1016/S0092-8674(00)80453-5

Kristan, D.M. 2007. Chronic calorie restriction increases susceptibility of laboratory mice (Mus musculus) to a primary intestinal parasite infection. *Aging Cell.* 6:817–825. http://dx.doi.org/10.1111/j.1474-9726.2007.00345.x

Lee, M.H., and H.Y. Yang. 2001. Negative regulators of cyclin-dependent kinases and their roles in cancers. *Cell. Mol. Life Sci.* 58:1907–1922. http://dx.doi.org/10.1007/PL00000826

Liu, L., and T.A. Rando. 2011. Manifestations and mechanisms of stem cell aging. *J. Cell Biol.* 193:257–266. http://dx.doi.org/10.1083/jcb.201010131

Liu, Y., S.E. Elf, Y. Miyata, G. Sashida, Y. Liu, G. Huang, S. Di Giandomenico, J.M. Lee, A. Deblasio, S. Menendez, et al. 2009. p53 regulates hematopoietic stem cell quiescence. *Cell Stem Cell.* 4:37–48. http://dx.doi.org/10.1016/j.stem.2008.11.006

Loewenthal, L.A., and W. Montagna. 1955. Effects of caloric restriction on skin and hair growth in mice. *J. Invest. Dermatol.* 24:429–433. http://dx.doi.org/10.1038/jid.1955.58

Longo, V.D., and M.P. Mattson. 2014. Fasting: molecular mechanisms and clinical applications. *Cell Metab.* 19:181–192. http://dx.doi.org/10.1016/j.cmet.2013.12.008

López-Lluch, G., N. Hunt, B. Jones, M. Zhu, H. Jamieson, S. Hilmer, M.V. Cascajo, J. Allard, D.K. Ingram, P. Navas, and R. de Cabo. 2006. Calorie restriction induces mitochondrial biogenesis and bioenergetic efficiency. *Proc. Natl. Acad. Sci. USA.* 103:1768–1773. http://dx.doi.org/10.1073/pnas.0510452103

Lyra, J.S., K. Madi, C.T. Maeda, and W. Savino. 1993. Thymic extracellular matrix in human malnutrition. *J. Pathol.* 171:231–236. http://dx.doi.org/10.1002/path.1711710312

Mackall, C.L., T.J. Fry, and R.E. Gress. 2011. Harnessing the biology of IL-7 for therapeutic application. *Nat. Rev. Immunol.* 11:330–342. http://dx.doi.org/10.1038/nri2970

Mattison, J.A., G.S. Roth, T.M. Beasley, E.M. Tilmont, A.M. Handy, R.L. Herbert, D.L. Longo, D.B. Allison, J.E. Young, M. Bryant, et al. 2012. Impact of caloric restriction on health and survival in rhesus monkeys from the NIA study. *Nature.* 489:318–321. http://dx.doi.org/10.1038/nature11432

Mattson, M.P. 2005. Energy intake, meal frequency, and health: a neurobiological perspective. *Annu. Rev. Nutr.* 25:237–260. http://dx.doi.org/10.1146/annurev.nutr.25.050304.092526

Mihara, M., M. Hashizume, H. Yoshida, M. Suzuki, and M. Shiina. 2012. IL-6/IL-6 receptor system and its role in physiological and pathological conditions. *Clin. Sci.* 122:143–159. http://dx.doi.org/10.1042/CS20110340

Mittal, A., B. Woodward, and R.K. Chandra. 1988. Involution of thymic epithelium and low serum thymulin bioactivity in weanling mice subjected to severe food intake restriction or severe protein deficiency. *Exp. Mol. Pathol.* 48:226–235. http://dx.doi.org/10.1016/0014-4800(88)90059-7

Miyamoto, T., H. Iwasaki, B. Reizis, M. Ye, T. Graf, I.L. Weissman, and K. Akashi. 2002. Myeloid or lymphoid promiscuity as a critical step in hematopoietic lineage commitment. *Dev. Cell.* 3:137–147. http://dx.doi.org/10.1016/S1534-5807(02)00201-0

Morrison, S.J., A.M. Wandycz, K. Akashi, A. Globerson, and I.L. Weissman. 1996. The aging of hematopoietic stem cells. *Nat. Med.* 2:1011–1016. http://dx.doi.org/10.1038/nm0996-1011

Muller-Sieburg, C.E., R.H. Cho, L. Karlsson, J.F. Huang, and H.B. Sieburg. 2004. Myeloid-biased hematopoietic stem cells have extensive self-renewal capacity but generate diminished lymphoid progeny with impaired IL-7 responsiveness. *Blood.* 103:4111–4118. http://dx.doi.org/10.1182/blood-2003-10-3448

Ogilvy, S., D. Metcalf, C.G. Print, M.L. Bath, A.W. Harris, and J.M. Adams. 1999. Constitutive Bcl-2 expression throughout the hematopoietic compartment affects multiple lineages and enhances progenitor cell survival. *Proc. Natl. Acad. Sci. USA.* 96:14943–14948. http://dx.doi.org/10.1073/pnas.96.26.14943

Omodei, D., and L. Fontana. 2011. Calorie restriction and prevention of age-associated chronic disease. *FEBS Lett.* 585:1537–1542. http://dx.doi.org/10.1016/j.febslet.2011.03.015

Orford, K.W., and D.T. Scadden. 2008. Deconstructing stem cell self-renewal: genetic insights into cell-cycle regulation. *Nat. Rev. Genet.* 9:115–128. http://dx.doi.org/10.1038/nrg2269

Parrella, E., T. Maxim, F. Maialetti, L. Zhang, J. Wan, M. Wei, P. Cohen, L. Fontana, and V.D. Longo. 2013. Protein restriction cycles reduce IGF-1 and phosphorylated Tau, and improve behavioral performance in an Alzheimer's disease mouse model. *Aging Cell.* 12:257–268. http://dx.doi.org/10.1111/acel.12049

Passegué, E., A.J. Wagers, S. Giuriato, W.C. Anderson, and I.L. Weissman. 2005. Global analysis of proliferation and cell cycle gene expression in the regulation of hematopoietic stem and progenitor cell fates. *J. Exp. Med.* 202:1599–1611. http://dx.doi.org/10.1084/jem.20050967

Patchen, M.L., T.J. MacVittie, J.L. Williams, G.N. Schwartz, and L.M. Souza. 1991. Administration of interleukin-6 stimulates multilineage hematopoiesis and accelerates recovery from radiation-induced hematopoietic depression. *Blood.* 77:472–480.

Peck, M.D., G.F. Babcock, and J.W. Alexander. 1992. The role of protein and calorie restriction in outcome from Salmonella infection in mice. *JPEN J. Parenter. Enteral Nutr.* 16:561–565. http://dx.doi.org/10.1177/0148607192016006561

Peschon, J.J., P.J. Morrissey, K.H. Grabstein, F.J. Ramsdell, E. Maraskovsky, B.C. Gliniak, L.S. Park, S.F. Ziegler, D.E. Williams, C.B. Ware, et al. 1994. Early lymphocyte expansion is severely impaired in interleukin 7 receptor-deficient mice. *J. Exp. Med.* 180:1955–1960. http://dx.doi.org/10.1084/jem.180.5.1955

Qian, H., N. Buza-Vidas, C.D. Hyland, C.T. Jensen, J. Antonchuk, R. Månsson, L.A. Thoren, M. Ekblom, W.S. Alexander, and S.E. Jacobsen. 2007. Critical role of thrombopoietin in maintaining adult quiescent hematopoietic stem cells. *Cell Stem Cell.* 1:671–684. http://dx.doi.org/10.1016/j.stem.2007.10.008

Qiu, X., K. Brown, M.D. Hirschey, E. Verdin, and D. Chen. 2010. Calorie restriction reduces oxidative stress by SIRT3-mediated SOD2 activation. *Cell Metab.* 12:662–667. http://dx.doi.org/10.1016/j.cmet.2010.11.015

Ritz, B.W., and E.M. Gardner. 2006. Malnutrition and energy restriction differentially affect viral immunity. *J. Nutr.* 136:1141–1144.

Rossi, D.J., D. Bryder, J.M. Zahn, H. Ahlenius, R. Sonu, A.J. Wagers, and I.L. Weissman. 2005. Cell intrinsic alterations underlie hematopoietic stem cell aging. *Proc. Natl. Acad. Sci. USA.* 102:9194–9199. http://dx.doi.org/10.1073/pnas.0503280102

Shimokawa, I., Y. Higami, G.B. Hubbard, C.A. McMahan, E.J. Masoro, and B.P. Yu. 1993. Diet and the suitability of the male Fischer 344 rat as a model for aging research. *J. Gerontol.* 48:B27–B32. http://dx.doi.org/10.1093/geronj/48.1.B27

Song, Z., J. Zhang, Z. Ju, and K.L. Rudolph. 2012. Telomere dysfunctional environment induces loss of quiescence and inherent impairments of hematopoietic stem cell function. *Aging Cell.* 11:449–455. http://dx.doi.org/10.1111/j.1474-9726.2012.00802.x

Spaulding, C.C., R.L. Walford, and R.B. Effros. 1997a. The accumulation of non-replicative, non-functional, senescent T cells with age is avoided in calorically restricted mice by an enhancement of T cell apoptosis. *Mech. Ageing Dev.* 93:25–33. http://dx.doi.org/10.1016/S0047-6374(96)01808-8

Spaulding, C.C., R.L. Walford, and R.B. Effros. 1997b. Calorie restriction inhibits the age-related dysregulation of the cytokines TNF-α and IL-6 in C3B10RF1 mice. *Mech. Ageing Dev.* 93:87–94. http://dx.doi.org/10.1016/S0047-6374(96)01824-6

Suda, T., F. Arai, and S. Shimmura. 2005. Regulation of stem cells in the niche. *Cornea.* 24:S12–S17. http://dx.doi.org/10.1097/01.ico.0000178742.98716.65

Suda, T., K. Takubo, and G.L. Semenza. 2011. Metabolic regulation of hematopoietic stem cells in the hypoxic niche. *Cell Stem Cell.* 9:298–310. http://dx.doi.org/10.1016/j.stem.2011.09.010

Sun, J., A. Ramos, B. Chapman, J.B. Johnnidis, L. Le, Y.J. Ho, A. Klein, O. Hofmann, and F.D. Camargo. 2014. Clonal dynamics of native haematopoiesis. *Nature.* 514:322–327. http://dx.doi.org/10.1038/nature13824

Thissen, J.P., J.M. Ketelslegers, and L.E. Underwood. 1994. Nutritional regulation of the insulin-like growth factors. *Endocr. Rev.* 15:80–101.

Thorén, L.A., K. Liuba, D. Bryder, J.M. Nygren, C.T. Jensen, H. Qian, J. Antonchuk, and S.E. Jacobsen. 2008. Kit regulates maintenance of quiescent hematopoietic stem cells. *J. Immunol.* 180:2045–2053. http://dx.doi.org/10.4049/jimmunol.180.4.2045

Ugochukwu, N.H., and C.L. Figgers. 2007. Caloric restriction inhibits up-regulation of inflammatory cytokines and TNF-α, and activates IL-10 and haptoglobin in the plasma of streptozotocin-induced diabetic rats. *J. Nutr. Biochem.* 18:120–126. http://dx.doi.org/10.1016/j.jnutbio.2006.03.008

von Freeden-Jeffry, U., P. Vieira, L.A. Lucian, T. McNeil, S.E. Burdach, and R. Murray. 1995. Lymphopenia in interleukin (IL)-7 gene-deleted mice identifies IL-7 as a nonredundant cytokine. *J. Exp. Med.* 181:1519–1526. http://dx.doi.org/10.1084/jem.181.4.1519

Walford, R.L., D. Mock, R. Verdery, and T. MacCallum. 2002. Calorie restriction in biosphere 2: alterations in physiologic, hematologic, hormonal, and biochemical parameters in humans restricted for a 2-year period. *J. Gerontol. A Biol. Sci. Med. Sci.* 57:B211–B224. http://dx.doi.org/10.1093/gerona/57.6.B211

Walter, D., A. Lier, A. Geiselhart, F.B. Thalheimer, S. Huntscha, M.C. Sobotta, B. Moehrle, D. Brocks, I. Bayindir, P. Kaschutnig, et al. 2015. Exit from dormancy provokes DNA-damage-induced attrition in haematopoietic stem cells. *Nature.* 520:549–552. http://dx.doi.org/10.1038/nature14131

Wang, J., H. Geiger, and K.L. Rudolph. 2011. Immunoaging induced by hematopoietic stem cell aging. *Curr. Opin. Immunol.* 23:532–536. http://dx.doi.org/10.1016/j.coi.2011.05.004

Warr, M.R., M. Binnewies, J. Flach, D. Reynaud, T. Garg, R. Malhotra, J. Debnath, and E. Passegué. 2013. FOXO3A directs a protective autophagy program in haematopoietic stem cells. *Nature.* 494:323–327. http://dx.doi.org/10.1038/nature11895

Wilson, A., E. Laurenti, G. Oser, R.C. van der Wath, W. Blanco-Bose, M. Jaworski, S. Offner, C.F. Dunant, L. Eshkind, E. Bockamp, et al. 2008. Hematopoietic stem cells reversibly switch from dormancy to self-renewal during homeostasis and repair. *Cell.* 135:1118–1129. http://dx.doi.org/10.1016/j.cell.2008.10.048

Yilmaz, O.H., R. Valdez, B.K. Theisen, W. Guo, D.O. Ferguson, H. Wu, and S.J. Morrison. 2006. Pten dependence distinguishes haematopoietic stem cells from leukaemia-initiating cells. *Nature.* 441:475–482. http://dx.doi.org/10.1038/nature04703

Yilmaz, O.H., P. Katajisto, D.W. Lamming, Y. Gültekin, K.E. Bauer-Rowe, S. Sengupta, K. Birsoy, A. Dursun, V.O. Yilmaz, M. Selig, et al.. 2012. mTORC1 in the Paneth cell niche couples intestinal stem-cell function to calorie intake. *Nature.* 486:490–495. http://dx.doi.org/http://dx.doi.org/10.1038/nature11163

Yin, D., D. Tuthill, R.A. Mufson, and Y. Shi. 2000. Chronic restraint stress promotes lymphocyte apoptosis by modulating CD95 expression. *J. Exp. Med.* 191:1423–1428. http://dx.doi.org/10.1084/jem.191.8.1423

Yoshihara, H., F. Arai, K. Hosokawa, T. Hagiwara, K. Takubo, Y. Nakamura, Y. Gomei, H. Iwasaki, S. Matsuoka, K. Miyamoto, et al. 2007. Thrombopoietin/MPL signaling regulates hematopoietic stem cell quiescence and interaction with the osteoblastic niche. *Cell Stem Cell.* 1:685–697. http://dx.doi.org/10.1016/j.stem.2007.10.020

You, T., W.E. Sonntag, X. Leng, and C.S. Carter. 2007. Lifelong caloric restriction and interleukin-6 secretion from adipose tissue: effects on physical performance decline in aged rats. *J. Gerontol. A Biol. Sci. Med. Sci.* 62:1082–1087. http://dx.doi.org/10.1093/gerona/62.10.1082

Zhang, J., J.C. Grindley, T. Yin, S. Jayasinghe, X.C. He, J.T. Ross, J.S. Haug, D. Rupp, K.S. Porter-Westpfahl, L.M. Wiedemann, et al. 2006. PTEN maintains haematopoietic stem cells and acts in lineage choice and leukaemia prevention. *Nature.* 441:518–522. http://dx.doi.org/10.1038/nature04747

SUPPLEMENTAL MATERIAL

Tang et al., http://www.jem.org/cgi/content/full/jem.20151100/DC1

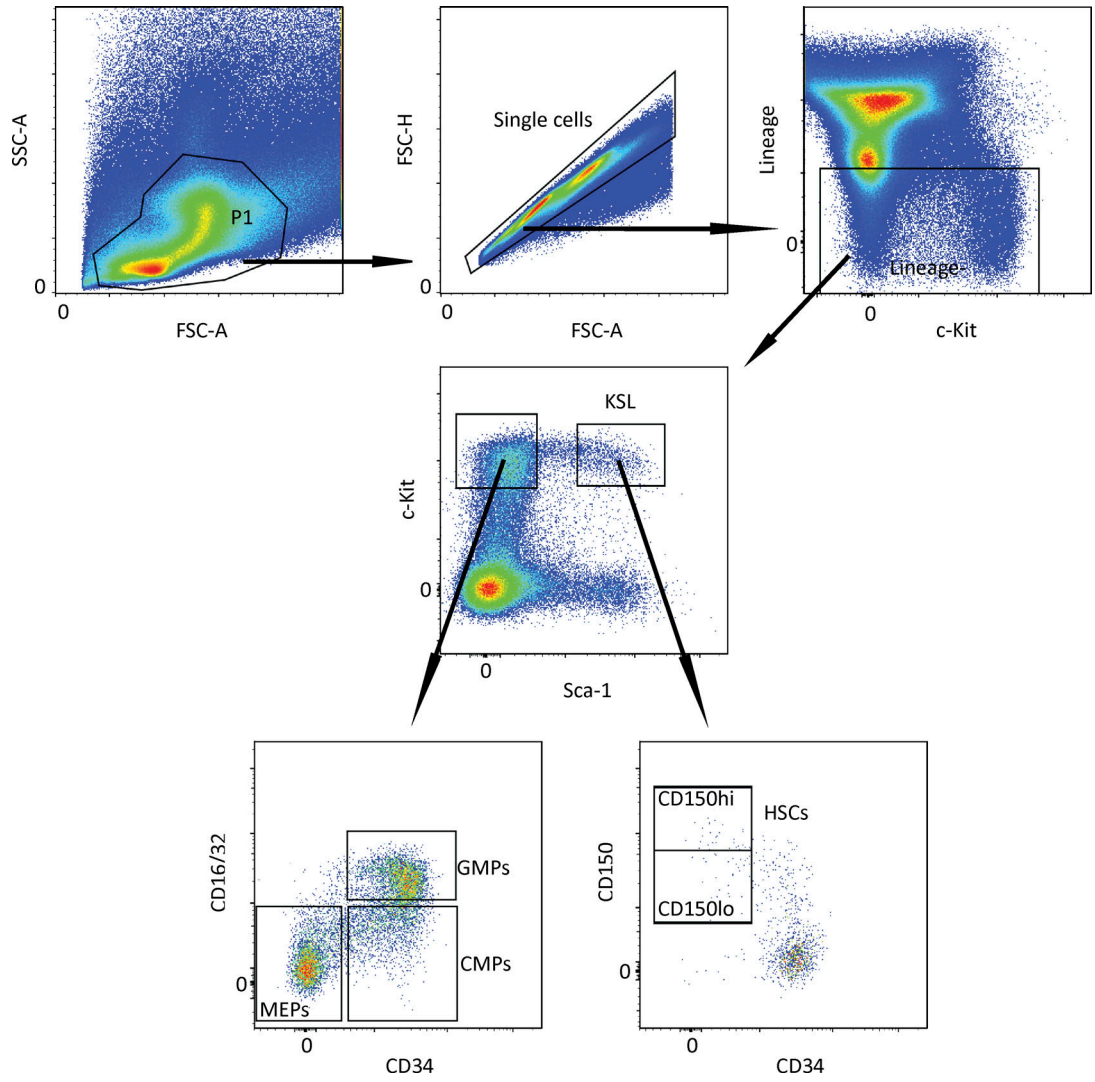

Figure S1. **Gating strategy of HSCs and myeloid/erythroid progenitors in flow cytometry analysis.**

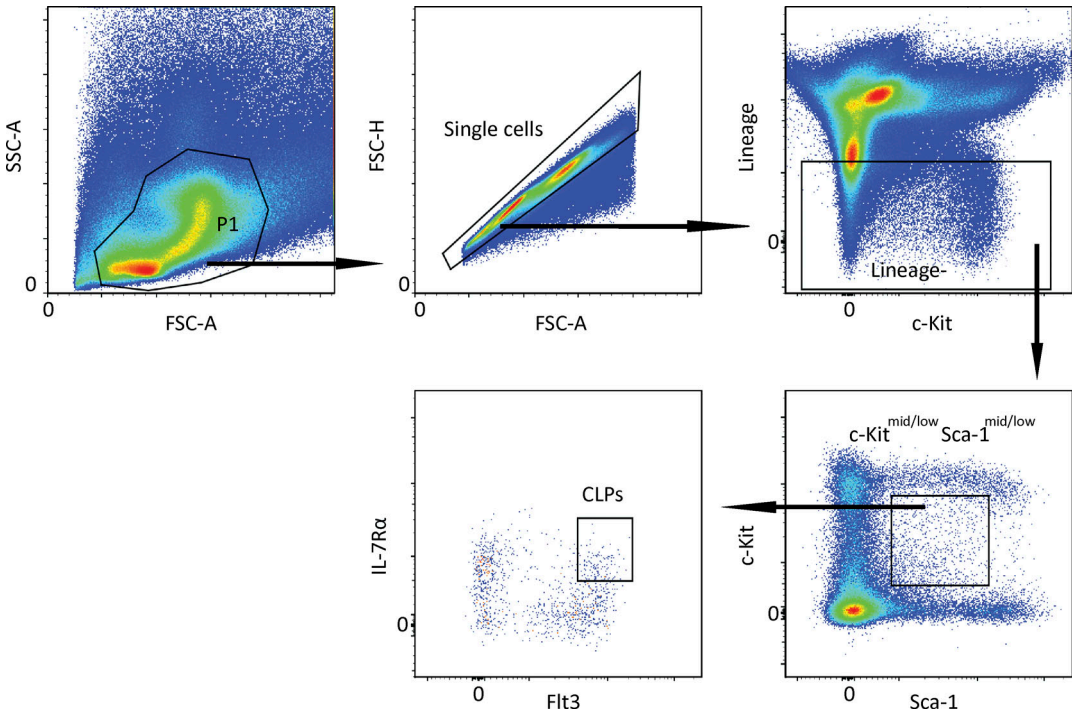

Figure S2. **Gating strategy of CLPs in flow cytometry analysis.**

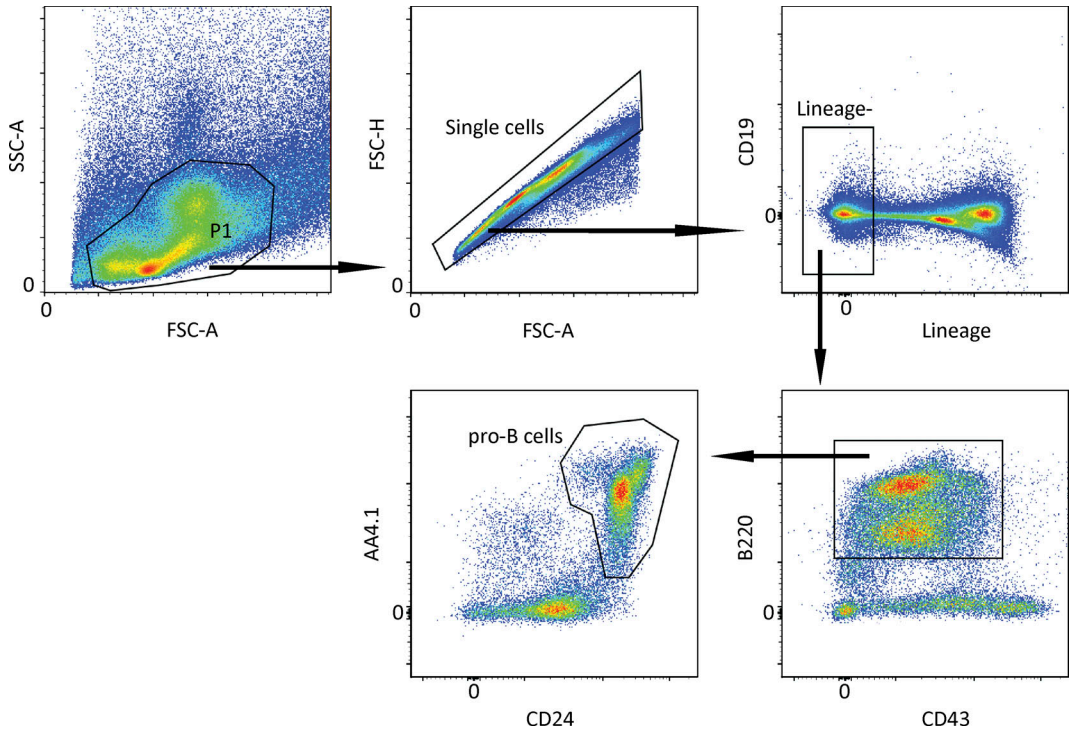

Figure S3. **Gating strategy of pro–B cells in flow cytometry analysis.**

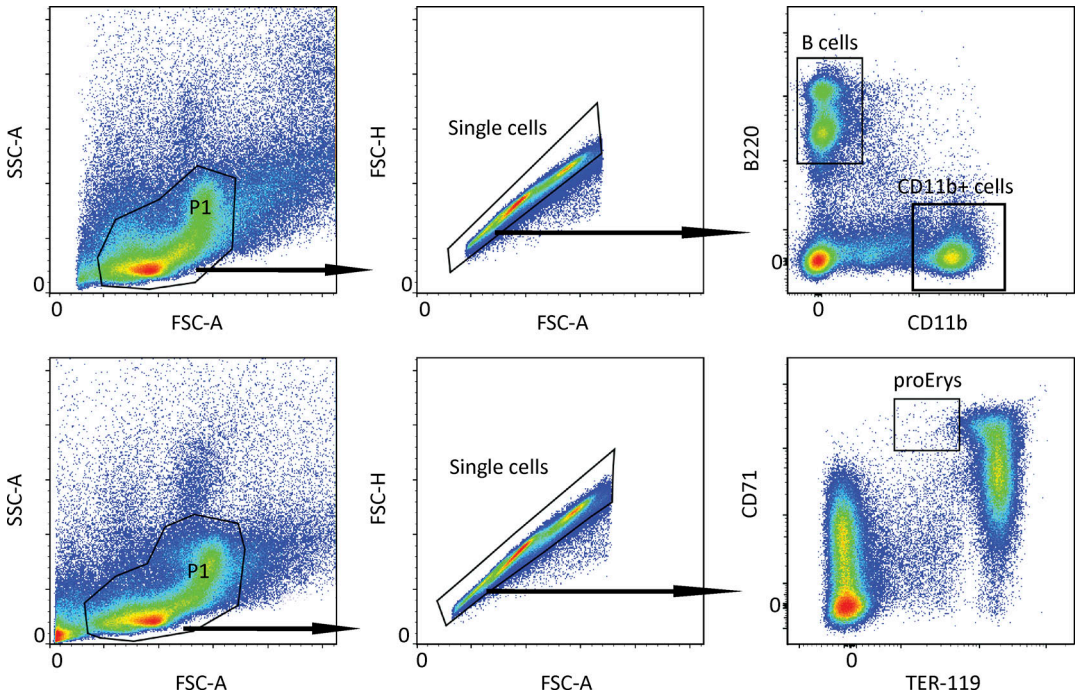

Figure S4. **Gating strategy of B cells, CD11b$^+$ cells, and proEry's in flow cytometry analysis.**